

Integrated drying and screening of small coal particles

GJW Dreyer

 orcid.org/0000-0003-1928-6793

Dissertation accepted in fulfilment of the requirements for the degree *Master of Engineering in Chemical Engineering* at the North-West University

Supervisor: Prof M le Roux

Co-supervisor: Prof QP Campbell

Graduation: May 2022

Student number: 25865722

DELIVERABLES FROM THIS STUDY

- **International conference (Presentation and article)**

Dreyer, G.J.W., Le Roux, M., Campbell, Q.P. 2021. Evaluating the dry screening performance of fine coal. *Conference proceedings*. Southern African Coal Processing Society International Coal Conference, Secunda, South Africa 12-14 October 2021. ISBN: 978-1-86822-715-0

SOLEMN DECLARATION

I, **Gert Jan Walt Dreyer**, hereby declare that the dissertation entitled,

“Integrated drying and screening of small coal particles”

which I hereby submit, in fulfilment of the requirements set for the degree Masters in Engineering at the North-West University, is my own individual work and has not previously been submitted to another institute.

Signed at Potchefstroom



Gert Jan Walt Dreyer

10 December 2021

Date

ACKNOWLEDGEMENTS

I want to give thanks to the North-West University for giving me the opportunity to further my studies. Furthermore, I would like to specifically thank the following persons/institutions for the support they offered me throughout this journey:

- To Coaltech Research Association. Thank you for the opportunity and your financial support.
- To my supervisor, Prof Marco le Roux, and my co-supervisor, Prof Quentin Campbell. Thank you for all the support and guidance throughout my studies and thank you for entrusting me with this opportunity. It was an honour to form a part of your team and contribute towards your larger research plan.
- To Mr Adrian Brock and the rest of the workshop staff. Thank you for all the hours of hard work to fix and modify the screen and, more than that, thank you for the support and coffee during long hours in the labs.
- To Mmes Sanet Botes and Simone Peacock. Thank you for managing and helping with the financial side of the project.
- To Ina-Lize Venter. Thank you for the professional language editing.
- To my friend and, in some ways, my mentor – Franco van de Venter. Thank you for your friendship, valuable advice and support. Without you, this project would have taken a lot longer.
- To my parents, Chris and Marietjie Dreyer. Thank you for the opportunities I have received and, furthermore, thank you for setting an example and always loving and supporting me, even when times were tough.
- To my wife, Anansa Dreyer. Thank you for your love and support when I most needed it. Thank you for being the one person that is always there for me.

This work is based on the research supported by the South African Research Chairs Initiative of the Department of Science and Technology and the National Research Foundation of South Africa (Chair Grant No: 86880, UID 85643, Grant No: 85632 and Grant UID 72310). Any opinion, finding, conclusion, or recommendation expressed in this material is that of the author(s) and the NRF accepts no liability in this regard.

ABSTRACT

The recent development of dry beneficiation technologies were motivated by the shortage of water, not only in South Africa, but in many other coal producing countries worldwide. The low capital and operating costs associated with dry coal beneficiation are made even more attractive by the added benefit of saving water. However, a drawback of dry coal beneficiation is the lower achievable efficiencies in relation to wet beneficiation. It is therefore important to maximize the cleaning efficiency of the various dry processes. One way of improving these techniques is finding an efficient dry screening method that would enable a plant to limit the particle size range sent to the dry beneficiation processes, and thus enable these units to operate on more focussed size ranges. Most of the current problems experienced with dry screening are caused by excess surface moisture on the coal particles, which causes particle agglomeration and ineffective screening.

The addition of an airflow system or ceramic pre-drying to a standard linear dry screen could improve its efficiency by reducing surface moisture and therefore the influence of the surface moisture on the particles during screening. Allowing fine agglomerated particles to separate from the parent particle.

To test this theory, a three-panel linear screen was equipped with an air-blow system at the bottom of the screen, and a dust collection system at the top. A standard coal feed was prepared from crushed and screened coal particles in the -6 mm to +0.5 mm range. The feed was moisture controlled to be at inherent, 5% and 10% moisture content. The prepared coal was fed to the modified screen at different bed depths, subjected to various airflow rates, and pre-dried using ceramic adsorbents in different mass ratios. The efficiency of the process was determined through particle size analysis of the feed, oversize stream and undersize stream, as well as measuring the moisture content of each stream.

During the determination of the undersize efficiency of screening -6 mm +0.5 mm ($d_{50} = 3.2$ mm) coal particles at screen aperture sizes of 5.6 mm and 2.8 mm the influence of surface moisture on the screening efficiency of the fine coal particles was also tested. An undersize efficiency of 70% was achieved when feeding the 5.6 mm aperture screen with coal at inherent moisture content. The undersize efficiency reduced to only 48% when the aperture of the screen was changed to 2.8 mm. It highlighted the difficulty of dry screening finer coal particles. With the feed coal at 5% surface moisture, the undersize efficiencies for the 5.6 mm and 2.8 mm aperture screens was found to be 68% and 12% respectively, with the greatest effect on particles of 2.8 mm and smaller. At 10% surface moisture in the feed, the undersize efficiency was below 20%

for the 5.6 mm apertures and below 4% for the 2.8 mm apertures, with all particles affected by agglomeration. These results clearly demonstrated the detrimental influence of surface moisture on screening efficiencies. This influence was also exaggerated at deeper bed depths. To increase the screening efficiency of the coal, air was blown from beneath the screen panels to assist in drying the coal and loosen the agglomerates. Under all specified conditions the addition of airflow did not improve the efficiency. The airflow did not have a significant impact on the moisture content of the coal due to the short contact time during screening.

A new feed had to be created that was in the -4 mm + 0.5 mm size range to allow easy separation of the 5 mm ceramics by screening. The new feed had a d_{50} of 1.92 mm. The undersize screening efficiency reduced from 90% at inherent moisture conditions with the new feed to 31% with the addition of 5% moisture content by weight, and to as low as 2% with the addition of 10% moisture content by weight. However, increased screening performance was observed when mixing the feed with ceramic adsorbents prior to feeding the coal with the ceramics to the screen. When using a 1:1 ceramic to coal mass ratio, the undersize efficiency increased to 83% with only 30 seconds of contact prior to screening at 5% moisture content, and to 85% with a 0.5:1 ceramic to coal mass ratio. When screening the adapted feed at 10% moisture content, the efficiencies were increased to 70% and 65% when using a 1:1 ceramic-to-coal mass ratio and a 0.5:1 ceramic-to-coal mass ratio respectively with 30 seconds of contact time. It was determined that contact time was the limiting factor for the reduction of moisture content. This was confirmed by increasing the contact time when screening at 10% moisture content to 120 seconds. The 1:1 ceramic-to-coal mass ratio undersize screening efficiency increased to 89% and the 0.5:1 ceramic-to-coal mass ratio to 86%.

In conclusion the airflow did not have any significant impact on the screening efficiency. This was due to too little contact time for the airflow to remove excess surface moisture which is the main cause of ineffective screening. The ceramic adsorbents however improved the screening efficiency by rapidly reducing excess surface moisture prior to and during screening.

Keywords: coal, fine coal, coal separation, dry screening, air-assisted screening, moisture reduction, ceramic adsorbents, ceramic pre-drying

TABLE OF CONTENTS

DELIVERABLES FROM THIS STUDY	I
SOLEMN DECLARATION	II
ACKNOWLEDGEMENTS	III
ABSTRACT	IV
CHAPTER 1: INTRODUCTION	1
1.1 Background and motivation	1
1.2 Scope of investigation	4
1.3 Research Aim and Objectives	4
1.3.1 Aim	4
1.3.2 Objectives.....	4
1.4 Dissertation outline	5
CHAPTER 2: LITERATURE REVIEW	6
2.1 Introduction to coal	6
2.1.1 Coal properties	6
2.1.2 Coal moisture content.....	7
2.1.3 Coal particle agglomeration	9
2.2 Coal Processing	9
2.2.1 Origin of coal processing	9
2.2.2 Wet processing of coal	9
2.2.3 Dry processing of coal	10
2.3 Screening of coal	11

2.3.1	Screen application and design	11
2.3.2	Vibrating screen capacity and efficiency	12
2.3.3	Dry screening of coal	13
2.3.4	Dry screening technology	14
2.3.5	Reduction of surface moisture by airflow	15
2.3.6	Reduction of surface moisture by adsorbents	16
2.3.7	Summary	17
CHAPTER 3: RESEARCH METHODOLOGY		18
3.1	Materials	18
3.1.1	Coal	18
3.1.2	Ceramic adsorbents	18
3.2	Experimental setup	19
3.2.1	Screening	19
3.3	Experimental design	21
3.3.1	Feed preparation	21
3.3.2	Screening	22
3.3.3	Analyses	23
3.4	Calculations	24
CHAPTER 4: RESULTS		26
4.1	Dry screening of small coal particles	26
4.1.1.1	Basis for screening efficiency when using 5.6 mm aperture size panels	26
4.1.1.2	Basis for screening efficiency using 2.8 mm aperture size panels	27

4.1.2	Influence of moisture	28
4.1.2.1	Influence of moisture when using 5.6 mm aperture size panels	28
4.1.2.2	Influence of moisture when using 2.8 mm aperture size panels	30
4.1.3	Influence of bed depth	32
4.1.3.1	Influence of bed depth using 5.6 mm aperture size panels	32
4.1.3.2	Influence of bed depth when using 2.8 mm aperture size panels.....	34
4.2	Dry screening with airflow	35
4.2.1	Effect of added airflow when using 5.6 mm aperture size panels.....	35
4.2.2	Effect of added airflow when using 2.8 mm aperture size panels.....	37
4.3	Ceramic pre-drying of coal	38
4.3.1	Basis for screening using the adapted feed	38
4.3.2	Influence of ceramic pre-drying.....	39
4.3.3	Influence of bed depth	42
4.3.4	Influence of contact time.....	44
4.3.5	Concluding remarks.....	46
CHAPTER 5: CONCLUSION, RECOMMENDATION AND CONTRIBUTION.....		47
5.1	Conclusion.....	47
5.2	Recommendation	48
5.3	Contribution.....	49
BIBLIOGRAPHY.....		50
ANNEXURES.....		54
6.1	Appendix 6.A.....	54

6.2 **Appendix 6.B..... 55**

6.3 **Appendix 6.C..... 56**

6.4 **Appendix 6.D..... 57**

6.5 **Appendix 6.E..... 58**

LIST OF TABLES

Table 3.1: Proximate analyses and calorific value results as received..... 18

Table 3.2: Composition and physical properties of the 5 mm spherical adsorbents 19

LIST OF FIGURES

Figure 1.1 Cumulative rainfall in South Africa for the 2020-2021 season (South African Weather Service, 2021)	1
Figure 1.2 Cumulative rainfall in South Africa for 2015-2016 season (South African Weather Service, 2021)	2
Figure 1.3: 24-month standard precipitation index for January 2019 to December 2020 (South African Weather Service, 2020:12)	2
Figure 2.1: Composition of coal (Dai <i>et al.</i> , 2020:103348)	7
Figure 2.2: Types of surface moisture associated with coal (Karthikeyan <i>et al.</i> , 2009:404).....	8
Figure 2.3: Typical application of different vibrating screens (Chen <i>et al.</i> , 2019:137).....	11
Figure 2.4: Illustration of forces acting on particles during elastic surface screening with impact balls (Duan <i>et al.</i> , 2020:117)	15
Figure 2.5: Typical drying curve of hygroscopic material by airflow (Barbosa de Lima <i>et al.</i> , 2016:21).....	16
Figure 2.6: Mechanism of adsorbent drying (Peters, 2016:22).....	17
Figure 3.1: Photo of the screen used with a) the total screen and b) the airflow system added to the bottom.	20
Figure 3.2: Photo of the panels used with a) the 5.6 mm panels and b) the 2.8 mm panels.....	20
Figure 3.3 Particle size distribution of the feed coal	21
Figure 3.4: Particle size distribution of the feed coal for ceramic experiments	22
Figure 3.5: Bed depths during operation a) Bed depth 1 b) Bed depth 2 c) Bed depth 3.....	23
Figure 3.6: Photographs of a) the oven used and b) the sieve shaker used.....	24
Figure 4.1: Undersize efficiencies for basis dry screening using 5.6 mm aperture size panels	26

Figure 4.2: Undersize efficiencies for basis dry screening using 2.8 mm aperture size panels	27
Figure 4.3: Undersize efficiencies when screening the standard feed with varying moisture contents using 5.6 mm aperture size panels	28
Figure 4.4: Efficiency analysis for each particle size range for basis screening with varying moisture contents using a 5.6 mm aperture size panel.....	29
Figure 4.5: Photograph showing agglomeration of wet particles to the screen surface	30
Figure 4.6: Undersize efficiencies when screening the standard feed with varying moisture contents using a 2.8 mm aperture size panel	30
Figure 4.7: Undersize efficiency analysis for each particle size range for basis screening with varying moisture contents using a 2.8 mm aperture size panel	31
Figure 4.8: Undersize efficiencies for basis screening with varying bed depths using 5.6 mm aperture size panels.....	32
Figure 4.9: Efficiency analysis for each particle size range with varying bed depth using 5.6 mm aperture size panels and 5% moisture content	33
Figure 4.10: Efficiency analysis for each particle size range with varying bed depth using 5.6 mm aperture panels at 10% moisture content	33
Figure 4.11: Undersize efficiencies for varying bed depths and moisture using 2.8 mm aperture size panels.....	34
Figure 4.12: Efficiency analysis for each particle size range with varying bed depth using 2.8 mm aperture size panels at 5% moisture content.....	35
Figure 4.13: Undersize efficiencies with varying airflow rates when using 5.6 mm aperture size panels.....	36
Figure 4.14: Undersize efficiencies with vary airflow rates when using 2.8 mm aperture size panels.....	37
Figure 4.15: Efficiency analysis for each particle size range for basis screening of adapted feed.....	38
Figure 4.16: Undersize efficiencies with addition of ceramics in different mass ratios.....	39

Figure 4.17: Efficiency analysis for each particle size range with the addition of ceramic adsorbents when screening at 5% moisture content	40
Figure 4.18: Efficiency analysis for each particle size range with the addition of ceramic adsorbents when screening at 10% moisture content	41
Figure 4.19: Undersize efficiencies with varying bed depths with the addition of a 1:1 ceramic to coal mass ratio.....	42
Figure 4.20: Undersize efficiencies with varying bed depths with the addition of a 0.5:1 ceramic to coal ratio	43
Figure 4.21: Undersize efficiencies with varying contact times and ceramic to coal mass ratios	44
Figure 4.22: Efficiency analysis for each particle size range for varying contact times using a 1:1 ceramic-to-coal mass ratio	45
Figure 4.23: Efficiency analysis for each particle size range for varying contact times using a 0.5:1 ceramic-to-coal mass ratio	45
Figure 6.1: Efficiency analysis for each particle size range for basis screening at a low bed depth.....	54
Figure 6.2: Efficiency analysis for each particle size range for basis screening at a high bed depth.....	54
Figure 6.3: Efficiency analysis for each particle size range for basis screening using 2.8 mm aperture size panels at a low bed depth	55
Figure 6.4: Efficiency analysis for each particle size range for basis screening using 2.8 mm aperture size panels at a high bed depth.....	55
Figure 6.5: Efficiency analysis for each particle size range using the adapted feed at a low bed depth.....	56
Figure 6.6: Efficiency analysis for each particle size range using the adapted feed at a high bed depth	56
Figure 6.7: Efficiency analysis for each particles size using the adapted feed with the addition of ceramics at 5% moisture content and a low bed depth	57

Figure 6.8: Efficiency analysis for each particle size range using the adapted feed with the addition of ceramics at 5% moisture content and a high bed depth 57

Figure 6.9: Efficiency analysis for each particles size range using the adapted feed at 10% moisture content and a low bed depth..... 58

Figure 6.10: Efficiency analysis for each particles size range using the adapted feed at 10% moisture content and a high bed depth 58

CHAPTER 1: INTRODUCTION

Chapter 1 provides the background and motivation of the research. It also determines the scope of the investigation, along with stating the aim and objectives of this study. The chapter is then concluded with the layout of the remainder of the dissertation.

1.1 Background and motivation

South Africa is a water scarce country and changes in weather patterns have caused a further reduction in rainfall. This produces uncertainty of what the future of water in South Africa holds. The projected rainfall for the country remains uncertain despite the scope of current research on the topic (Department of Environmental Affairs, 2013:53). The average rainfall from 1981-2010 was calculated to be 598 mm with a high concentration of rain in the eastern coastal areas of the country. As a result, large parts of the country are considered arid regions (South Africa Weather Service, 2020:6). The 2020-2021 season saw above average rainfall, but there are still arid regions (see Figure 1.1).

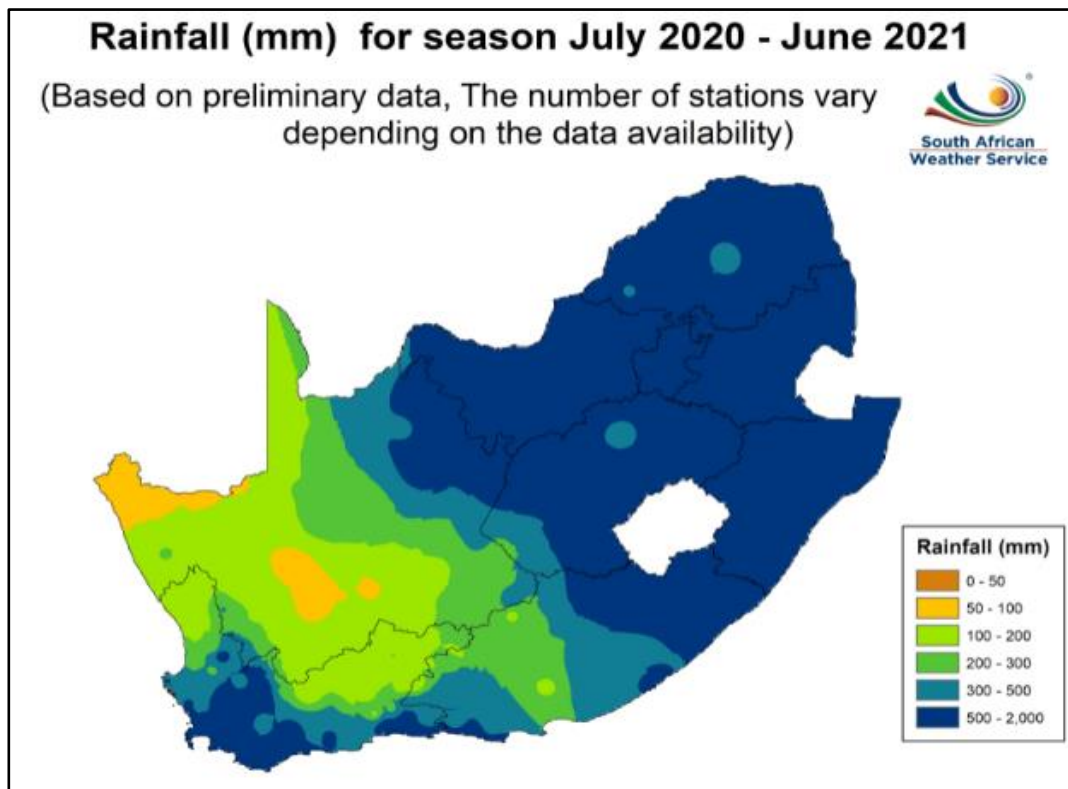


Figure 1.1 Cumulative rainfall in South Africa for the 2020-2021 season (South African Weather Service, 2021)

It is clear that the rainfall for this season was above average when compared to the 2015-2016 season in Figure 1.2, where many areas with coal reserves received less than 500 mm of rain.

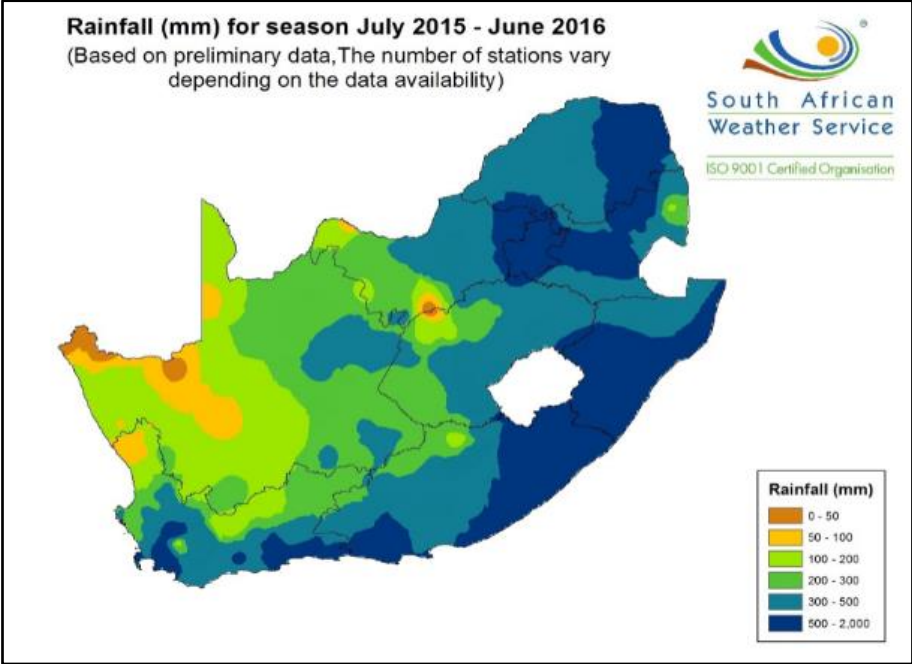


Figure 1.2 Cumulative rainfall in South Africa for 2015-2016 season (South African Weather Service, 2021)

The areas that received less than 500 mm run the risk of experiencing droughts, which could result in a process water shortage if dry conditions such as these occur for extended periods of time. Figure 1.3 shows the 24-month standard precipitation index, which is useful for identifying areas of drought.

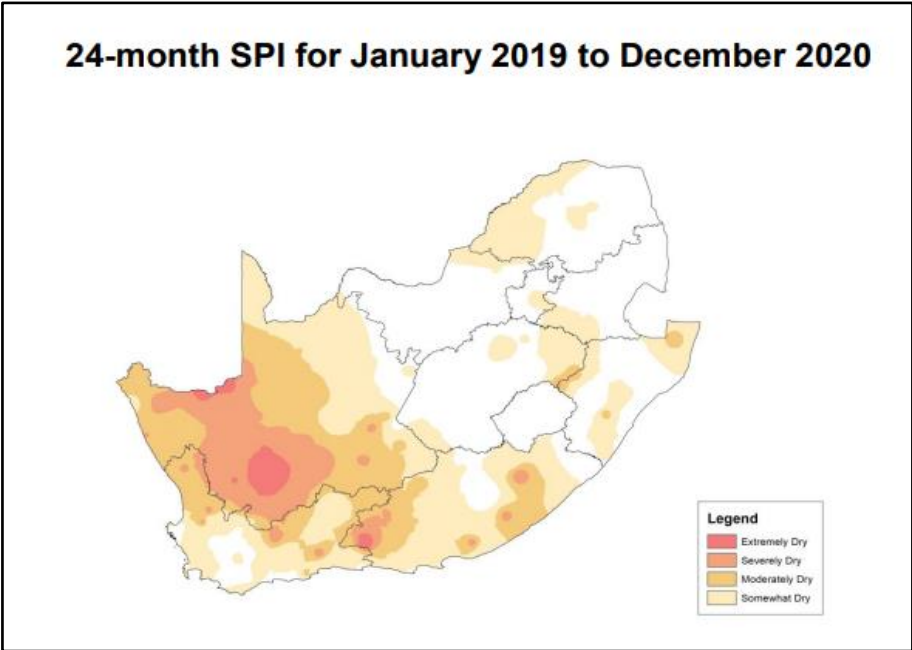


Figure 1.3: 24-month standard precipitation index for January 2019 to December 2020 (South African Weather Service, 2020:12)

The index in Figure 1.3 can be linked to streamflow, reservoir levels, and groundwater levels (South African Weather Service, 2020:12). In Figure 1.3, it can be seen that many areas with coal reserves are experiencing somewhat dry conditions, even with good rainfall over the past 5 years. The shortage of water – especially process water used in beneficiation plants – and the uncertain future has brought a sense of urgency to the development and improvement of methods of dry beneficiation.

A lot of research work has been done on different techniques and equipment for dry beneficiation, but most of these techniques and equipment cannot process a large range of particle sizes in one single unit. Each one of these units usually has the ability to process a 1:3 particle size range (Peng *et al.*, 2015:209).

The screening of coal is therefore a very important step in the beneficiation cycle, as beneficiation technologies require a specific particle size range to operate effectively. In current wet processes, spray water is used on the screens to increase the efficiency of size separation. It requires large amounts of water to be sprayed through nozzles onto the coal bed in order to remove the agglomerated fine coal particles from the surface of the larger ones. The use of water to remove fine particles in dry processing is impossible for obvious reasons (Peng *et al.*, 2015:210). The addition of spray water to increase the screening efficiency would necessitate large amounts of capital and operational costs post screening to dry the coal. Hence, effective dry screening of small coal particles will help utilize newly developed dry beneficiation processes more effectively.

Limited research has been conducted on dry screening. The research that has been published shows that the largest contributor to low screening efficiencies for small coal dry processing is excess surface moisture. This causes a tendency for fine run of mine material to attach to screen surfaces and agglomerate to oversize particles, resulting in a reduction of screening efficiency, screen open area, and aperture blinding (Kaza *et al.*, 2019:8). The surface moisture is concentrated on small coal particles due to the larger surface area relative to mass. The mass of the particles determines the forces exerted on it during screening and therefore the larger coal particles are easily screened, but small particles with high moisture contents and small masses are difficult to screen. It can therefore be hypothesized that limiting the excess surface moisture in the small particles should, in theory, reduce problems experienced with dry screening small coal particles.

1.2 Scope of investigation

The scope of this investigation is focused on increasing the efficiency of dry screening with a linear vibrating screen by reducing the surface moisture content of the feed coal. A laboratory scaled two panel linear vibrating screen was used during the experimental work. Two primary methods of reducing the surface moisture were implemented, namely the addition of an airflow system, and the addition of ceramic adsorbents to the coal prior to feeding the screen. The following operational variables were included:

1. Coal surface moisture content (inherent, 5% and 10%)
2. Screen aperture size (5.6 mm and 2.8 mm)
3. Screen operating bed depth
4. Airflow rates (0, 200 and 360 l/min)
5. Ceramic adsorbent to coal mass ratio (1:1 and 0.5:1)

1.3 Research Aim and Objectives

1.3.1 Aim

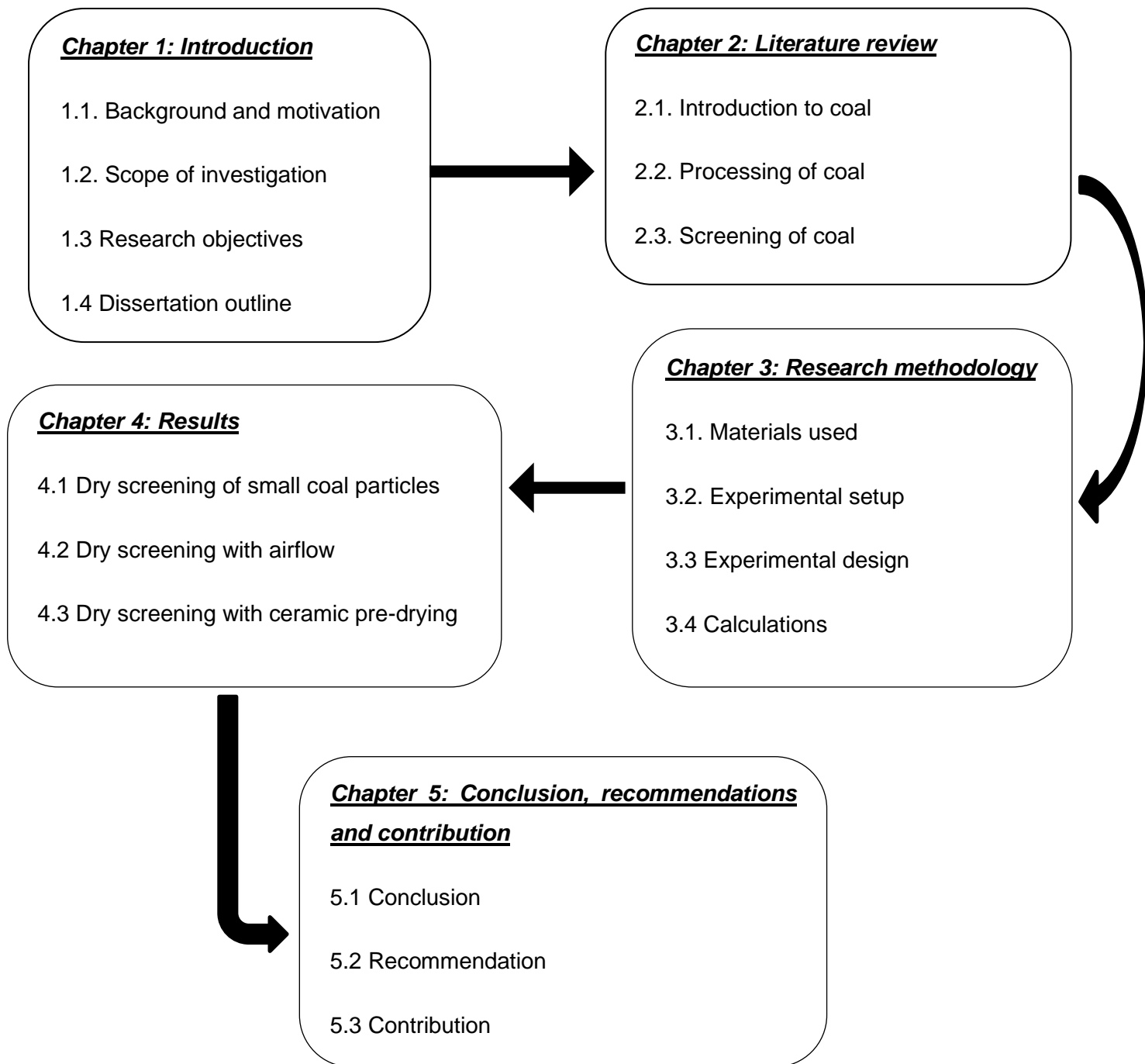
The aim of this study is to improve the dry screening efficiency of fine coal by controlling the influence of particle surface moisture.

1.3.2 Objectives

The following objectives were set for this study:

1. To modify and commission an existing two-panel screen with the addition of an airflow system and dust control capabilities.
2. To determine the effect of excess surface moisture on the dry screening efficiency of fine coal when using the linear vibrating screen.
3. To determine the effect forced airflow has on the screening efficiency and related coal product moisture.
4. To determine the effect of pre-mixing ceramic adsorbents into the coal feed and measuring the screening efficiency thereof.
5. Analyse the influence of bed depth on the operation of the screen under all operating parameters.

1.4 Dissertation outline



CHAPTER 2: LITERATURE REVIEW

In this literature study, a short introduction to coal is given, which discusses the properties of coal, the moisture content of coal, as well as the agglomeration of particles in fine coal. This is followed by an explanation of coal processing and the necessity of dry processing of coal. The final part of the literature study is about the screening of coal, which includes the dry screening of coal and the reduction of surface moisture content by air and adsorbents.

2.1 Introduction to coal

2.1.1 Coal properties

Coal can be described as complex combustible sedimentary rock that consists mostly of aquatic plant debris and other plant materials that were primarily deposited as peat and secondarily as mud. Over time, physical and chemical changes were induced by heat and pressure at depths stretching from 1 to 6 kilometres below the surface to ultimately form coal (Bechtel *et al.*, 2013:59; He *et al.*, 2014:116). The formation of coal is much more complex than a mere mixture of organic chemicals and some minerals exposed to heat and pressure; it is a complex and dynamic living and metabolising mixture (Dai *et al.*, 2020:103348).

The properties of coal are determined by its origin and evolution and can be described by means of three parameters. These three parameters are organic geochemistry, inorganic geochemistry, and coal rank (Bechtel *et al.*, 2013:59).

The organic geochemistry of coal is determined by the origin of the organic materials. There are three main groups of organic material, namely vitrinite, liptinite and inertinite (Bechtel *et al.*, 2013:59). Vitrinite is derived from humic matter and is characterized by a grey colour that is darker than inertinite, but lighter than liptinites. The elemental composition of vitrinite changes with rank and is characterized by the following elemental ranges (ICCP, 1998:350):

- Carbon contents ranging from 77-96%
- Hydrogen contents of 1-6%
- Oxygen contents of 1-16%

Inertinite is composed of macerals from diverse origin including, tissues of fungi and higher plants, fine detrital fragments, gelified amorphous material and cell secretions altered by redox and biochemical processes during peatification. Inertinite is characterized by high carbon contents with low oxygen and hydrogen contents (ICCP, 2001:460). Liptinite is a group of macerals derived from humifiable plant matter that is relatively hydrogen rich, like sporopollenin, resins, waxes and fats (Cardott *et al.*, 2017:43).

The organic and inorganic geochemistry can be summarised as shown in Figure 2.1.

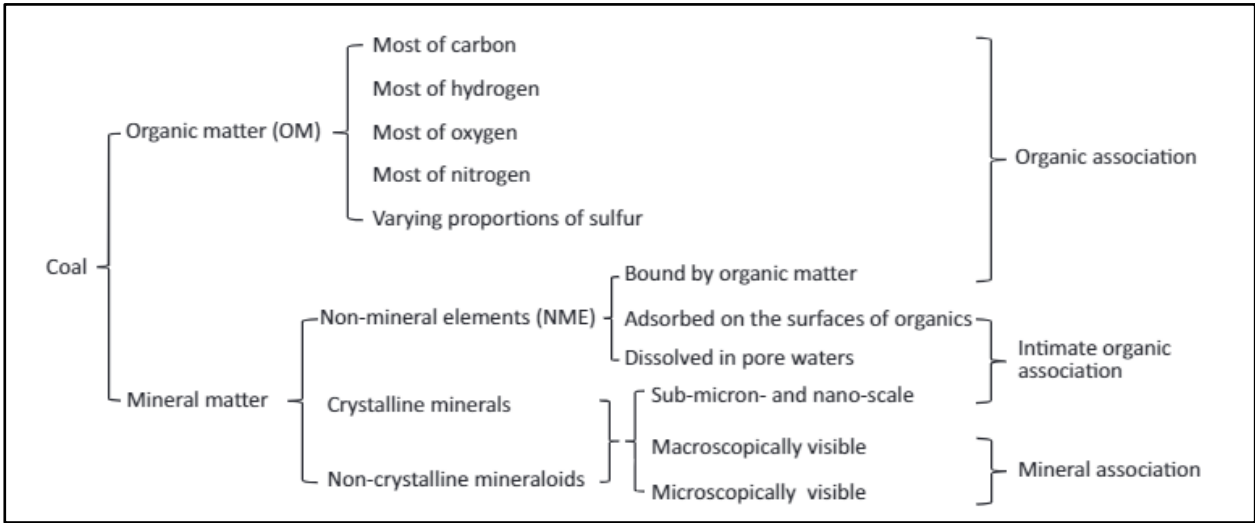


Figure 2.1: Composition of coal (Dai *et al.*, 2020:103348)

The summarised organic geochemistry shows that the most common elements in coal is carbon, hydrogen, oxygen and nitrogen. The inorganic geochemistry is broken up into three categories namely non-mineral elements, crystalline minerals, and non-crystalline mineraloids.

The inorganic geochemistry of coal is described as the presence of minerals such as oxides, trace elements and rare elements. These inorganic constituents originate from the detrital inputs of the swamp where peatification took place and also from chalcophile elements associated with sulphide minerals (Ameh, 2019:263).

Finally, coal rank describes the extent of metamorphic transformation in the macerals and minerals. This reflects the maximum temperature to which the coal has been exposed and also the time it was held at that temperature. It also reflects to a lesser extent the pressure regime through the time and temperature it was exposed to (Bechtel *et al.*, 2013:59). Coal is thus a complex sedimentary rock with multiple factors affecting its properties. These factors include its origin, heat, depth and also the presence of moisture.

2.1.2 Coal moisture content

The interaction between water and coal is somewhat unknown and complex. It is, however, widely accepted that the moisture in coal can be described as either bound moisture or free moisture (Han *et al.*, 2013:11). The free moisture is not influenced by the properties of the solid particles, but the bound moisture’s properties are modified by the presence of the solid particles (Cen *et*

al., 2014:122). The moisture in coal can be further divided into five sub-groups as described by Karthikeyan *et al.* (2009:404):

1. Interior adsorption water, which is contained within the micropores and microcapillaries in each coal particle and deposited during the formation of the coal particle.
2. Surface adsorption water forms a layer of water molecules on the surface of the coal particles.
3. Capillary water contained in the capillaries and small crevices within a single coal particle.
4. Interparticle water contained in the capillaries and small crevices between coal particles.
5. Adhesion water forms a layer or film of water around the surface of a single or agglomerated particle.

The five types of surface moistures can be illustrated as in Figure 2.2:

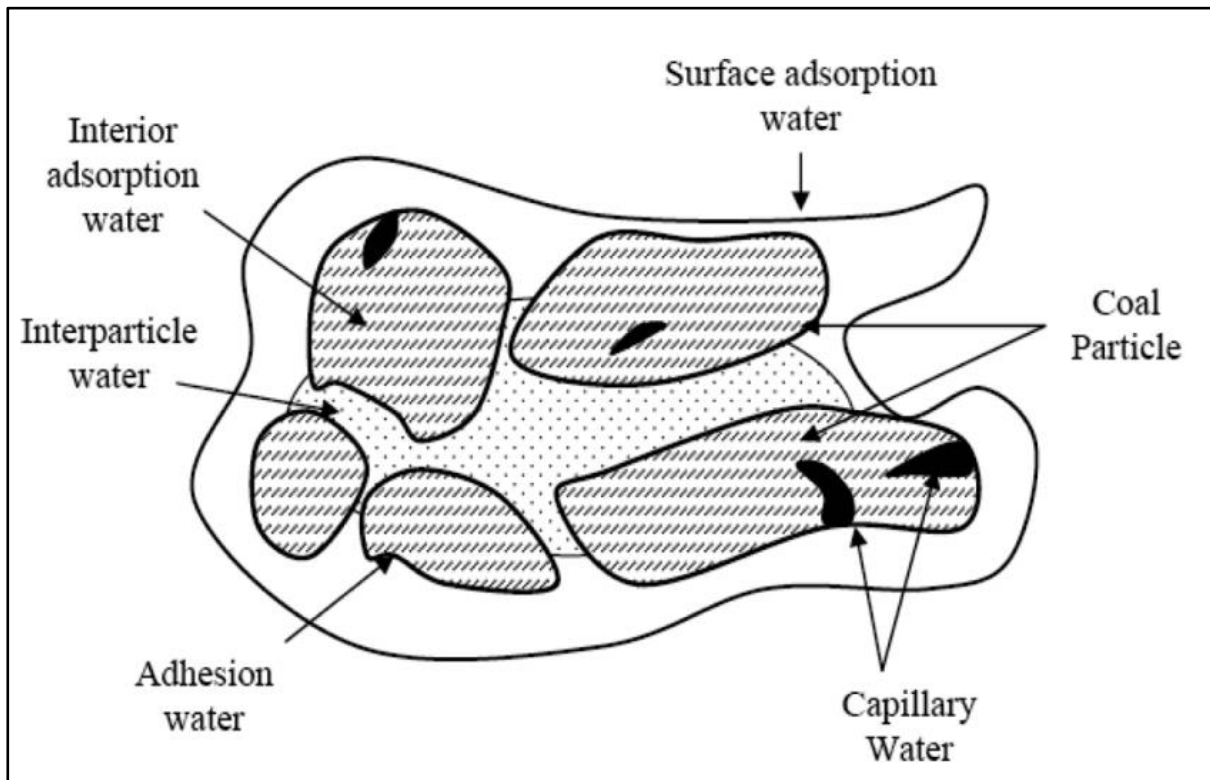


Figure 2.2: Types of surface moisture associated with coal (Karthikeyan *et al.*, 2009:404).

The complex interactions between coal and water are well described and illustrated by (Karthikeyan *et al.*, 2009:404). This creates a better understanding of the interaction and shows that coal particles can agglomerate due to the presence of excess surface moisture. The first two types of moisture are known as inherent moisture and can only be removed by thermal drying methods. Types 4 and 5 are known as surface moisture and can be removed by mechanical dewatering methods. Type 3 falls somewhere in between and can be partially removed by

mechanical methods depending on the size of the openings in the coal surface and the temperature of drying (Han *et al.*, 2013:11).

2.1.3 Coal particle agglomeration

The agglomeration of coal particles refers to the adhesion of one or more particles to each other. This agglomeration of coal particles is caused by excess moisture. The moisture causes the formation of coal pseudo-particles (Amaral *et al.*, 2019:241). In small coal particles, the voids become capillary cavities. These cavities are then filled with water, and the free drainage of the water is no longer possible, since the surface tension forces between the coal's surface and the water becomes larger than the forces exerted (Nokele, 2004:173). Capillary forces play an important role in the maintenance of the agglomerate structure and is therefore one of the main driving forces in the agglomeration of particles. The capillary pressure is influenced by the moisture content of the interparticle pore volume (Basha *et al.*, 2019:135). The agglomeration of fine coal particles cause numerous problems when processing coal with high moisture contents.

2.2 Coal Processing

2.2.1 Origin of coal processing

Coal preparation and beneficiation is one of the best methods to use coal resources efficiently and to decrease the environmental impact of coal mining (Duan *et al.*, 2015:100). There has been a general increase in the amount of low-grade ore being mined, which causes the creation of more fine coal. In addition, there has been an increase in the usage of mechanical equipment, which has also caused the production of more coal fines (De Korte, 2015:571). Plants in South Africa have reported that 6% of the ROM (run-of-mine) coal is -2 mm in size, and that fine and ultra-fine coal, which includes all -6 mm particles, contribute 11% of the total ROM (Campbell *et al.*, 2015:335). These factors have made it necessary to process coal. However, due to the use of water to remove fines and lower quality coal during the processing of coal, many plants discard these fines directly into tailings ponds (Ackah *et al.*, 2017:581)

2.2.2 Wet processing of coal

Most industrial applications use wet screening and processing methods. Wet screening methods can increase the surface moisture content of coal to as much as 12%, depending, on a variety of factors (Chen & Wei, 2003:52). The wet cleaning of coarse coal is very efficient, but the dewatering and cleaning of wet fine coal causes many problems, resulting in many plants directly discarding the particles smaller than 150 micrometres into tailings ponds. This results in a loss of clean usable coal and a loss of revenue, along with numerous environmental issues caused by the tailings ponds (Ackah *et al.*, 2017:581).

The most common environmental issues caused by tailings ponds include acid mine drainage, spontaneous combustion, and dust release as the coal is exposed to weathering (Campbell *et al.*, 2015:335). Not only is the water usage and discarding of fine coal a problem, but the product yielded by wet processing usually has a high moisture content, which exacerbates the difficulty of handling using the products (Lou *et al.*, 2017:439)

The Waterberg coalfield – one of the largest unmined coal fields in South Africa, containing 40-50% of the remaining coal resources – has been poorly developed in the past due to the shortage of water, which has made it very difficult to process and remove fines (Hartnady, 2010:3). This has led to the necessity of developing dry processing methods.

2.2.3 Dry processing of coal

Coal beneficiation technology has recently been developed with the purpose of saving water. Many successful methods and technologies have been developed using dry techniques. These technologies include air jigs, air tables, air-dense medium fluidized beds, and dry vibration fluidized beds. The low capital and operating cost of dry processing makes it an attractive option, but the low separation efficiency of the process could make it less attractive. There is an urgent necessity to develop and promote the use of dry beneficiation technology due to the scarcity of water in most regions that are rich in coal (Duan *et al.*, 2015:100). The dry beneficiation technologies that have already been implemented in South Africa include the FXG dry coal separator and X-ray sorting (De Korte, 2015:571). High efficiencies can be achieved for particles in the size range of 6-50 mm, but the separation of 6-1 mm coal is difficult to achieve by means of conventional fluidized beds (Duan *et al.*, 2015:100). The moisture content also has a negative effect on the efficiency of beneficiation.

The surface moisture of fine coal has an adverse effect on the dry beneficiation process. The efficiency of a vibrated gas-solid fluidized bed is affected negatively at free moisture contents as low as 2% by weight (Duan *et al.*, 2015:105). The restriction for most of these dry processing technologies is that they are limited to certain size ranges (Peng *et al.*, 2015:207). Fine coal has a much higher likelihood of absorbing moisture and can have moisture content of up to 25% by weight after filtration (Campbell *et al.*, 2015:335). As a result, the effective dewatering and sizing of fine coal would enable the fine coal to be beneficiated and added to the final product without affecting the quality of the final product and thus increasing the overall yield of processing plants.

2.3 Screening of coal

2.3.1 Screen application and design

The screening of coal is the basic method of sizing coal and also aids in the efficient utilization of coal resources. Screening is mainly achieved through a linear vibrating screen. Vibrating screens account for up to 33% of equipment at a modern coal preparation plant (Chen *et al.*, 2019:137). The typical application of different vibrating screens is described in Figure 2.3.

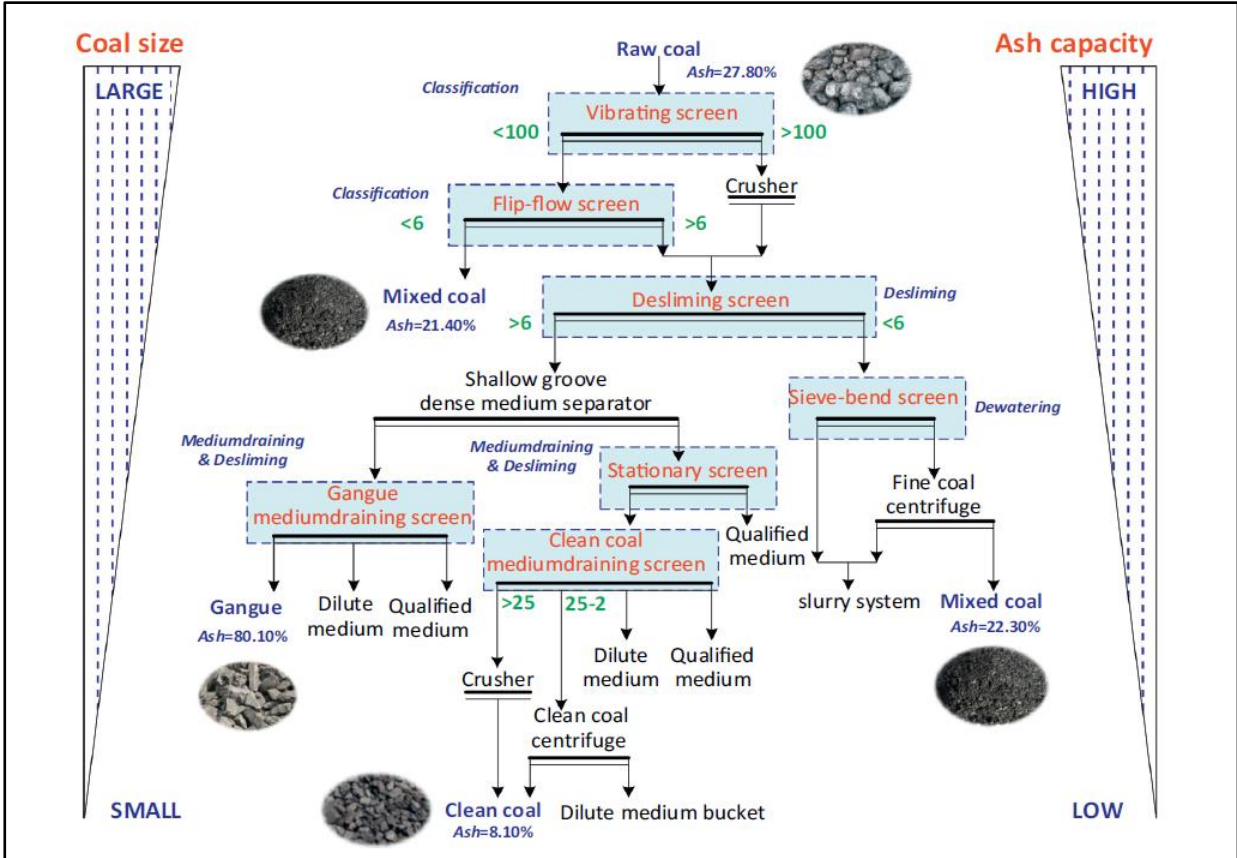


Figure 2.3: Typical application of different vibrating screens (Chen *et al.*, 2019:137)

As illustrated in Figure 2.3 the screening of fine coal is most commonly achieved by a flip-flow screen. These flip-flow screens usually use water to remove the fine coal particles, which – as discussed earlier – cause numerous environmental issues and issues for dry processing technologies.

2.3.2 Vibrating screen capacity and efficiency

There are numerous factors that influence screening efficiency of which one of the most important factors is the probability of a single particle to pass through the opening in the screen. The probability can be calculated by using the equation of A.M. Goden (Pelevin, 2020:1):

$$P = \varphi \left(\frac{a - d}{a} \right)^\psi = \varphi \left(1 - \frac{d}{a} \right)^\psi \quad 2.1$$

The equation takes into account the following factors:

- φ = The effective screening area
- d = The particle diameter (mm)
- a = Aperture size of the sieve (mm)
- ψ = Coefficient taking into account the shape of the sieve mesh

From this equation, it can be derived that, as the diameter of the particle approaches the diameter of the screen opening, the probability of that particle passing the screen reduces exponentially. The probability is further influenced by other factors as described by Sullivan (2013:18), which include material factors and machine factors.

The first material factor is the shape of the particle. The most common shapes include angular, spherical, acicular, ovaloid, flaky and slabby – all with different probabilities of passing that influence the screenability of the material. The density of the particles also has an influence on how the particle reacts to the screen surface and interacts with other particles. The third material factor is the moisture content of the particles. Surface moisture causes the agglomeration of particles, which reduces the probability of particles passing. The final material factor is the size distribution of the granular bulk material. The size distribution is determined by particle size distribution and is used as the basis for the calculation of screening efficiency.

The machine factors include the material, shape and size of the screen panels used. This changes the effective area of screening which, in turn, influences the efficiency. The second machine factor is the motion of the vibrating screen. The motion changes the rate at which material moves over the panels and the forces exerted on the particles. By doing this, it determines the number of presentations of each particle on the panels, thus influencing the probability of each particle to pass the screen. The motion of a vibrating screen can be optimized for each application by changing the amplitude (otherwise known as stroke length) and the frequency of the vibration.

To calculate the capacity of a screen all these factors have to be taken into account using factors. This can be achieved by using the equation as presented in (Sullivan, 2013:18):

$$A = \frac{F \times U}{100C_c \times K_1 \times K_2 \times K_3 \times K_4 \times K_5 \times K_6 \times K_7} \quad 2.2$$

Where:

- A = Screen area [m²]
- F = Feed rate [stph]
- U = Percentage undersize in feed
- C_c = Unit capacity [stph/m²]
- K₁ = Percentage half-size to the screen opening read off a standard graph
- K₂ = Bulk density/100
- K₃ = Particle shape factor
- K₄ = Deck location factor
- K₅ = Aperture shape factor
- K₆ = Open area factor
- K₇ = Bed depth correction factor

The efficiency of a screen is described as the weight percentage of undersize particles screened in a single screening to the total amount of undersize particles contained in the feed (Sullivan, 2013:28).

2.3.3 Dry screening of coal

One method of separating the coal particles into specific size ranges without the use of water is dry screening. This is a field that has not received a lot of attention, because of the low efficiencies achieved. The lack of efficiency in dry screening is due to particle agglomeration and screen blinding, which is a problem, especially if the feed coal has a high surface moisture content (Kaza *et al.*, 2019a:8).

There are two different types of screen blinding. The first type is the blocking of apertures by near graded particles and the second is the blocking of apertures by particles that have clogged together by means of agglomeration. These agglomerates adhere to the screen surface, resulting in the blocking of screen apertures. The moisture content has a great influence on the screening performance of coal. In the coal moisture content range of 8.9% - 13.7%, the adhesion between particles was strengthened with the increase in external moisture content, and the amount of fine particles adhering to the surface of coarse particles was increased (Duan *et al.*, 2020:113).

In a study on a new dry screen with an aperture size of 2 mm when screening fine coal of size range -3+1 mm, an efficiency of 86.0% was achieved with the following controlled variables. Varying moisture contents of 4-8%, varying screen angles of 1 to -3 degrees, and varying vibrational frequencies of 10Hz to 7Hz (Kaza *et al.*, 2019a:8). More studies were done on the same screen with different aperture sizes and different particle size ranges. The particle size ranges were -6+4 mm, -4+2 mm and -2+0.5 mm, and the aperture sizes were 5 mm, 3 mm and 1mm respectively for each particle size range. Each set of particle size ranges were tested and the optimum operational conditions were determined. For the -6+4 mm particles, the optimum conditions were a vibrational frequency of 10Hz and a screen angle of +2 degrees. The screen delivered an efficiency of 87.4%. For the -4+2 mm particle size range, the optimum conditions were 10Hz and +1 degree and an efficiency of 80.5% was achieved. For the final particle size range of -2+0.5 mm, the optimum conditions were 9Hz and a -1 degree screen angle, and the efficiency was 66.4% (Kaza *et al.*, 2019b:8).

2.3.4 Dry screening technology

In order to increase efficiency of dry screening and avoid aperture blinding, some researchers have tried to increase the vibration intensity of the screen to break agglomerated particles. This, however, increases the dynamic stress on the structure of the screen and results in easy damage and high failure rates, making it uneconomical for large-scale use. The flip-flow screen is an elastic screen surface used to increase the vibration intensity. The elastic screen surface enables the screen to withstand high vibration intensities and also causes the apertures to partially deform, allowing agglomerated particles to be broken (Dong *et al.*, 2017:93).

The flip-flow screen combines the flexible polyurethane-type screen with a new vibrating system, which results in up to 50 times more force of acceleration. This results in many advantages over traditional screens, such as less cleaning required, more uniform screening operation, higher screen capacity and efficiency, higher acceleration forces on particles, but low acceleration forces on screen body, less energy consumption and, finally, the use of wear resistant polyurethane panels (Ackah *et al.*, 2017:585).

Further development of the flexible screening partially solved the problem of screen plugging during flexible surface screening by the addition of hitting balls underneath the screen surface. The balls continually impact the screen and also the plugged particles aiding in the unplugging of the screen (Duan *et al.*, 2020:115). The forces acting in on the screen are illustrated in Figure 4.

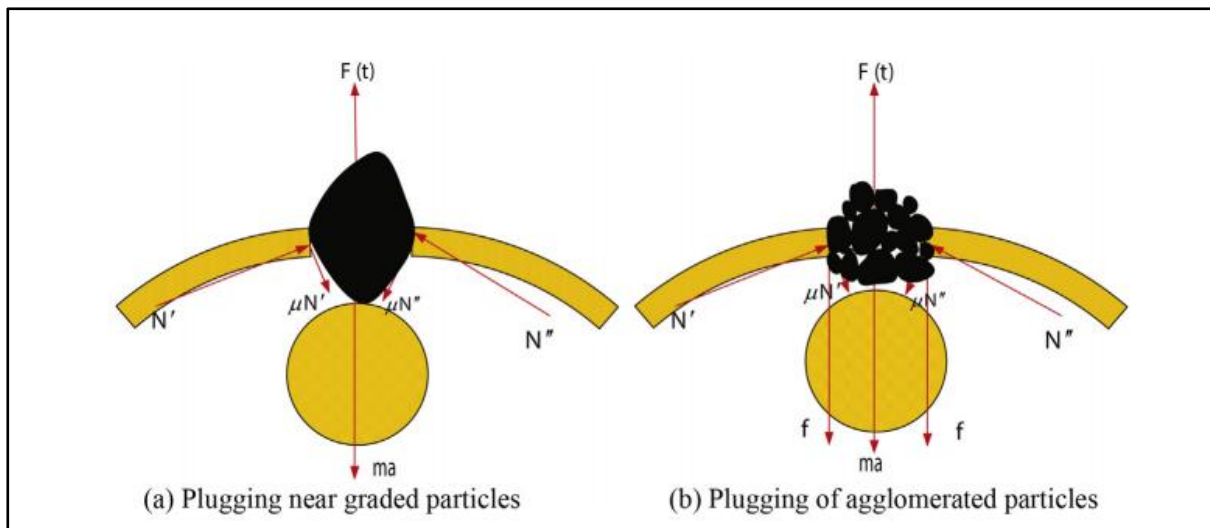


Figure 2.4: Illustration of forces acting on particles during elastic surface screening with impact balls (Duan *et al.*, 2020:117)

Figure 2.4 clearly illustrates the working principle of the impact balls creating a force on the screen and also the particles and, by doing so, unplugging the screen. The breaking of agglomerated particles can thus be achieved in two ways: the application of a force or the reduction of surface moisture, which reduces the binding force of agglomerated particles.

2.3.5 Reduction of surface moisture by airflow

Moisture transfer from coal to air is initiated by the unsaturated nature of air. Continuous airflow ensures that the coal is constantly in contact with unsaturated air. This results in the evaporation of moisture, and mass transfer from the coal particles to the air (Van Rensburg, 2019:25). The drying of coal through airflow can be separated into three stages as described by Barbosa de Lima *et al.* (2016:21). The three stages are also illustrated in Figure 2.5.

The first stage is the initial drying period, which is characterized by a large mass transfer caused by the large initial moisture concentration gradient. The easy removal of free moisture contributes to a rapid initial moisture removal.

The second stage is the constant rate period. The onset of this period is when some of the free moisture on the surface is removed causing the interparticulate moisture to migrate to the boundary layer at a constant rate. As this moisture reaches the surface, it is transferred to the airflow, resulting in the constant reduction of moisture until the interparticulate moisture is greatly reduced. During this period, the temperature of the material equals the wet bulb temperature.

The third stage is known as the falling rate period, and is the result of the complete removal of all free surface moisture, and marks the start of the removal of bounded moisture. Moisture has to migrate through capillaries, resulting in a slow rate of removal that decreases as the bounded

moisture content reduces. The temperature also starts increasing towards the temperature of the air as moisture is reduced.

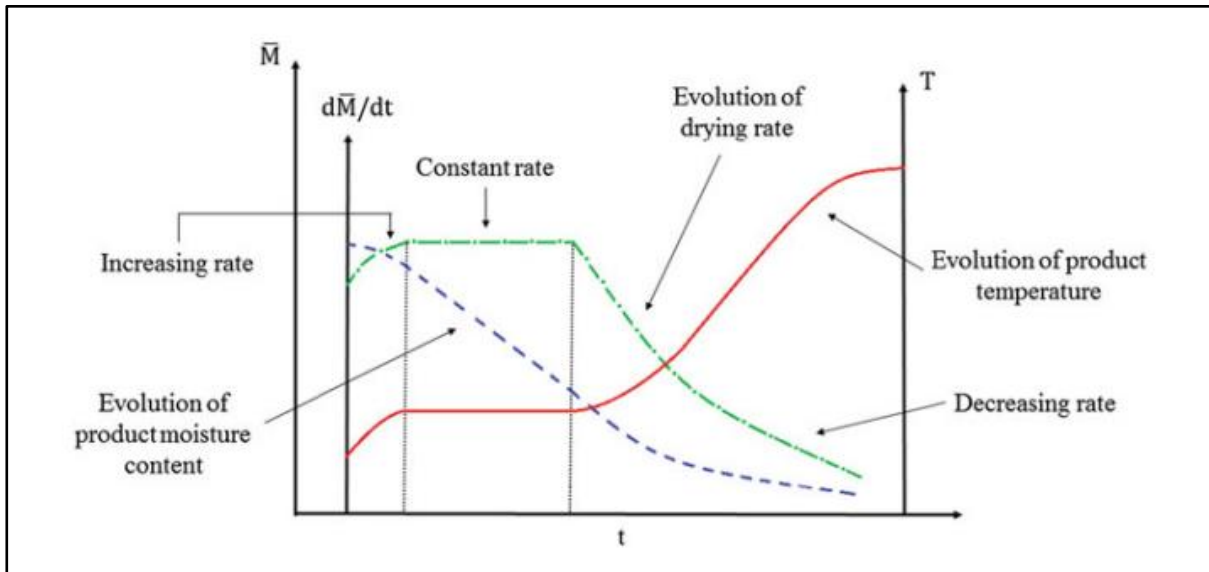


Figure 2.5: Typical drying curve of hygroscopic material by airflow (Barbosa de Lima *et al.*, 2016:21)

Laboratory results have shown that the surface moisture of -5 mm coal particles can be reduced by 10-15% by exposing them to a 1-minute airflow at a velocity of 0.6-1m/s (Ackah *et al.*, 2017:581). The main drive in the reduction of surface moisture seems to be relative humidity. Energy calculations have shown that the fluidization of fine and ultra-fine coal particles is more energy efficient than other thermal drying processes (Campbell *et al.*, 2015:338).

2.3.6 Reduction of surface moisture by adsorbents

Contact-sorption drying is described as the process of drying a wet material through contact with adsorbents. The method is complex and affected by many factors, such as the distinct phases of adsorption, multi-components systems, and thermal effects (Peters, 2016:21). Alumina-silicate adsorbents are highly porous and have a hydrophilic, hygroscopic nature, which makes the adsorption of liquid and vapour possible. During production, activated alumina is dehydrated, resulting in open active sites on the surface of the adsorbent to which water molecules can attach (Van Rensburg, 2019:28). Ceramics adsorb moisture from the wet material by capillary flow. The rate of adsorption is thus dependent on the contact area between the surface of the wet material and the adsorbent surface. The adsorption process can be separated into three phases as illustrated in Figure 2.6. The first stage is the transfer of mass from the surface of the wet material to the surface area of the adsorbent via capillary flow. This causes a reduction in available surface area as capillaries are filled with moisture. Once the flow of moisture through the boundary of particles decreases, the moisture continues to migrate to the core of the adsorbent, and from the core of the wet material to its surface. This results in a lower mass transfer rate of moisture from

material surface to adsorbent surface. After sufficient time has passed, no more mass transfer takes place from surface to surface, as the moisture in the core of the wet material reduces. If the adsorbents are not removed, a third stage is likely to occur in which the mass transfer might be reversed, as moisture is re-adsorbed from the adsorbent surface to the material surface due to the relative difference in surface moistures (Peters, 2016:21).

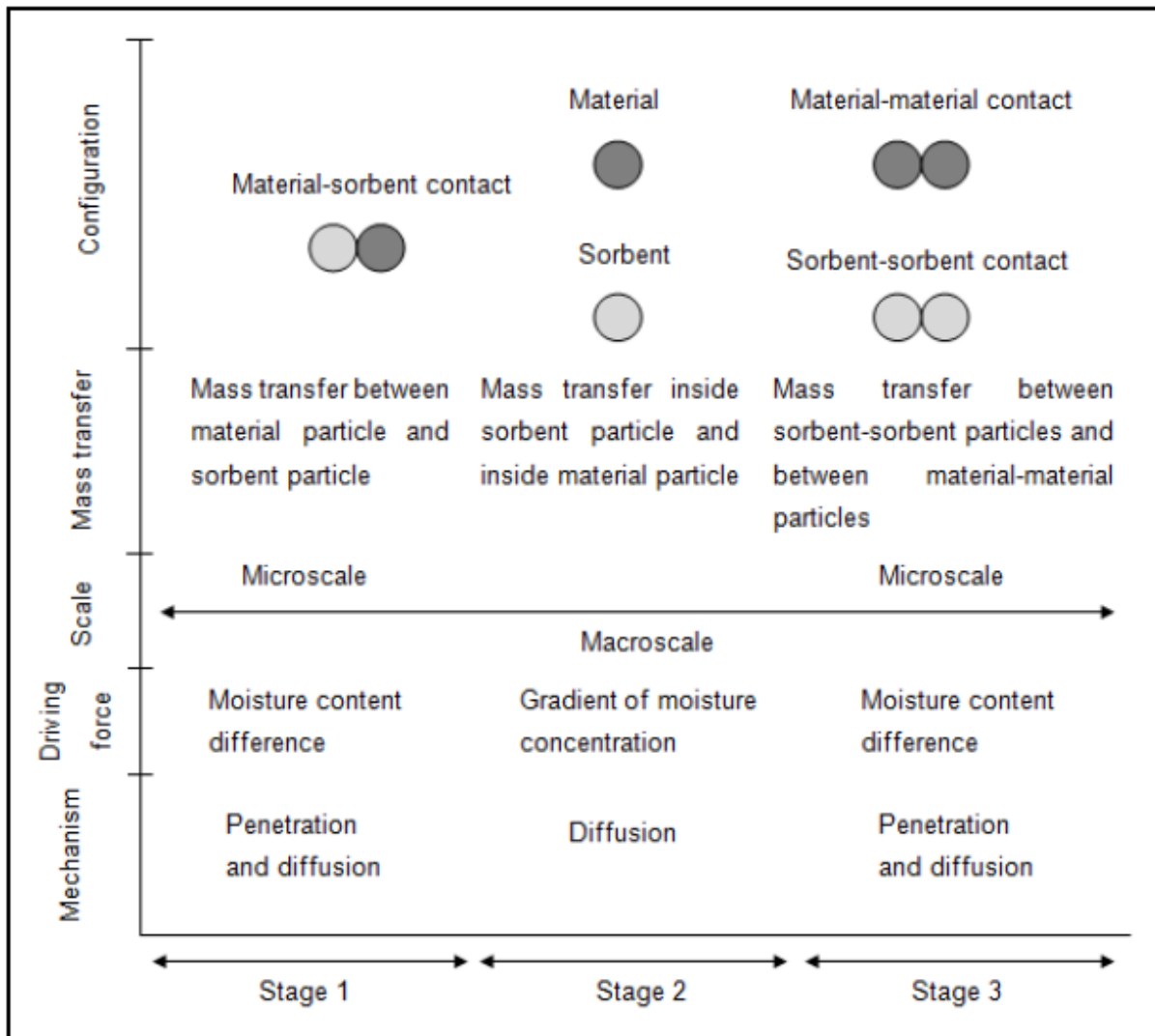


Figure 2.6: Mechanism of adsorbent drying (Peters, 2016:22)

2.3.7 Summary

The literature review covered many aspects of coal and coal screening including the influence of moisture on screening. The review also covered methods to increase the force exerted on the particles and other methods to break agglomerates, but there has been no literature found focusing on removing moisture prior to and during screening to increase efficiency which could be more efficient and cost effective.

CHAPTER 3: RESEARCH METHODOLOGY

The research methodology describes the materials and methods used to test the efficiency of dry screening and the impact of coal drying during screening and pre-screening. Two methods were used to dry the coal, namely airflow-enhanced screening and pre-drying by means of ceramic adsorbents.

3.1 Materials

3.1.1 Coal

The pre-prepared feed coal, which is ROM coal from Witbank Seam 5 in Mpumalanga, South Africa, was crushed and screened to predetermined size ranges of -6.7+4.8 mm, -4.0+2.0 mm and -2.0+0.5 mm.

The coal's characteristics as determined by proximate analysis are summarised in Table 3.1. The coal was used as received when conducting the proximate analysis. The coal was exposed to ambient air conditions for extended periods while crushing and screening took place, and therefore free moisture was limited.

Table 3.1: Proximate analyses and calorific value results as received

Proximate Analyses				
Sample	-6.7+4.8 mm	-4.0+2.0 mm	-2.0+0.5 mm	Test method standard
Inherent moisture	3.13% ± 0.16%	2.58% ± 0.07%	2.55% ± 0.04%	SANS 5925:2007
Volatiles	22.47% ± 0.43%	22.75% ± 0.59%	23.02% ± 0.14%	SANS 50:2011
Ash yield	42.19% ± 0.74%	51.92% ± 1.05%	51.31% ± 0.42%	SANS 131:2011
Fixed carbon	32.21% ± 1.33%	22.75% ± 1.16%	23.12% ± 2.21%	By difference
Calorific value [MJ/kg]	22.00 ± 0.006	22.37 ± 0.007	19.97 ± 0.007	ISO 1928: 2020
Sulphur content	1.00% ± 0.003%	1.00% + 0.006%	1.63% ± 0.015%	ISO 19579: 2006

3.1.2 Ceramic adsorbents

The adsorbents used are commercially available Porocel Dryocel 848 activated alumina ceramics used as received. The ceramics are spherical in shape and have a diameter of 5 mm. The composition and physical properties are listed in Table 3.2.

Table 3.2: Composition and physical properties of the 5 mm spherical adsorbents

Composition (Volatile-free Basis)	Al ₂ O ₃	93.5 %
	Na ₂ O	0.35 %
	SiO ₂	0.015 %
	H ₂ O	6.135 %
Physical properties	Surface Area	320 m ² / g
	Total Pore Volume	0.5 cm ³ / g
	Abrasion loss	0.2 % _{wt}
	Attrition (% Retained)	99.6 % _{wt}
	Crush Strength (5 mesh equivalent)	20 kg
	Bulk Density	753 kg/ m ³

3.2 Experimental setup

3.2.1 Screening

A laboratory scale three-panel linear vibrating screen, depicted in Figure 3.1a, was used in this study. The screen was modified by adding an airflow system underneath the screen panels as shown in Figure 3.1b. The airflow system consisted of a series of PVC pipes with equally spaced holes drilled into the top of the pipes. The system was coupled to the laboratory instrument airline while the airflow was controlled using an inline flowmeter and bypass valve to give 0 L/min, 200 L/min or 360 L/min.

When in operation, the screen had a stroke length of 4 mm, which resulted in an average retention time of 5 seconds for a single particle fed to the screen. For dust control purposes, the top of the screen was enclosed with a 2 mm plate fitted onto it. The plate is also visible in Figure 3.1a. The panels that were fit to the screen were procured from a local company and varied in aperture sizes to include 5.6 mm and 2.8 mm. The panels are shown in Figure 3.2a and b.

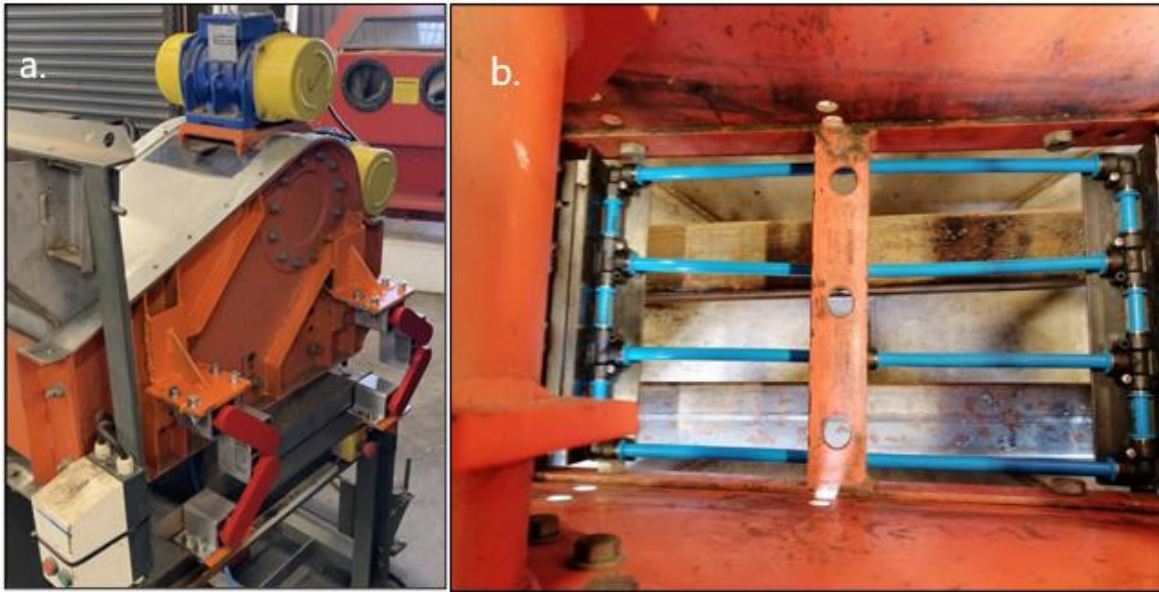


Figure 3.1: Photo of the screen used with a) the total screen and b) the airflow system added to the bottom.



Figure 3.2: Photo of the panels used with a) the 5.6 mm panels and b) the 2.8 mm panels

3.3 Experimental design

3.3.1 Feed preparation

A standard feed was prepared by adding the three coal feed size ranges of (-6.7+4.8 mm, -4+2 mm and -2+0.5 mm) together in mass ratios of 1:1:0.5 respectively, resulting in a cumulative passing fraction graph determined by particle size distribution analysis, as shown in Figure 3.3. It can be seen from the graph that it indicates a 100% passing of 6.7 mm with a d_{50} size of 3.2 mm. The specific ratio was used to ensure a standard feed close to what could be expected after crushing.

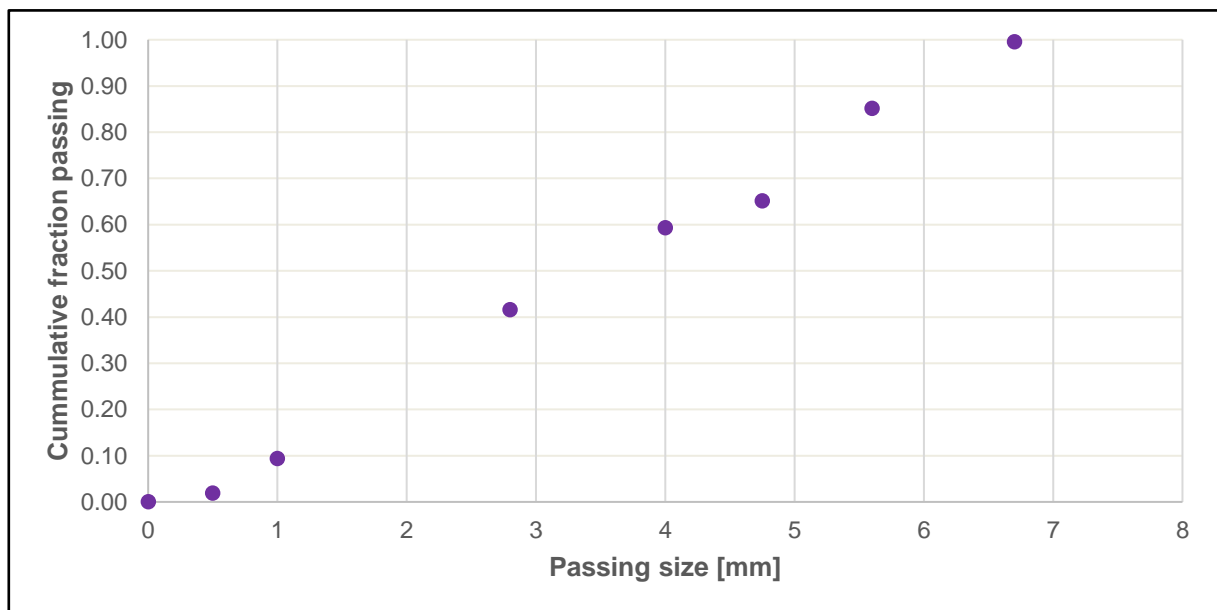


Figure 3.3 Particle size distribution of the feed coal

A second feed was prepared for experimentation, which included the use of ceramics. The feed was adapted to a 1:1 mass ratio of the -4.0+2.0 mm and the -2.0+0.5 mm size ranges to ensure easy separation of the 5 mm ceramics from the coal by screening with a 4 mm sieve. The new cumulative passing fraction graph is depicted in Figure 3.4. This graph indicates a 100% passing of 4 mm particles and a d_{50} size of 1.9 mm.

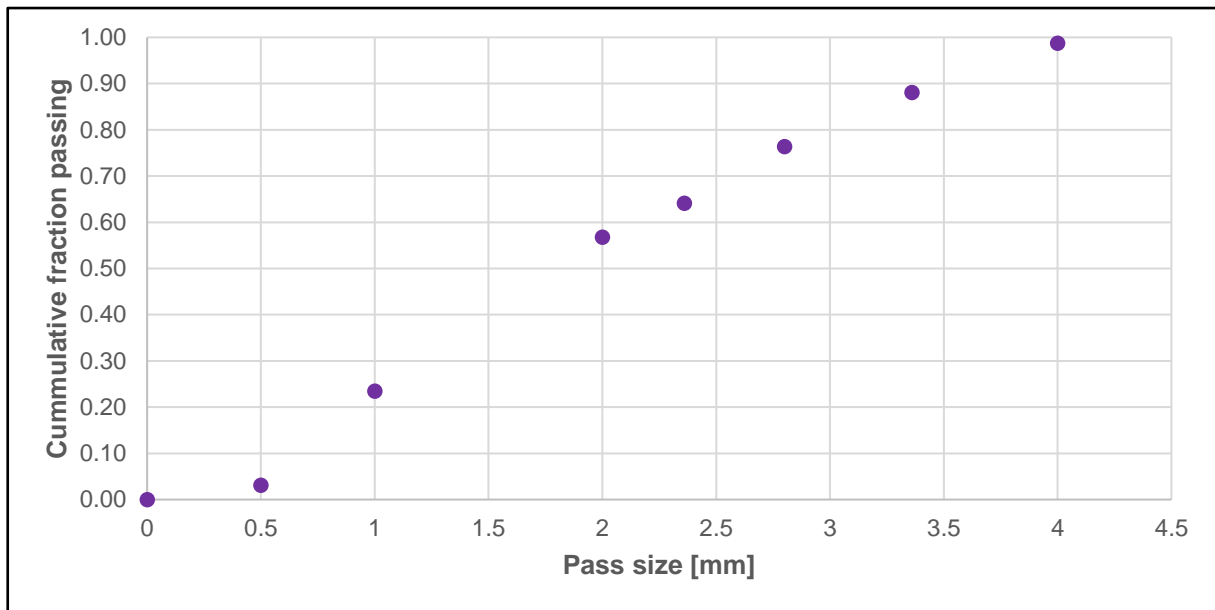


Figure 3.4: Particle size distribution of the feed coal for ceramic experiments

3.3.2 Screening

After creating the two different feed mixtures based on the particle size, sub-samples were prepared using a riffle splitter. The required masses depended on the bed depth at which the specific run should be done. The bed depths were a low bed depth (Bed depth 1, consisting of 500g material fed over 20 seconds), a medium bed depth (Bed depth 2, consisting of 1500g material fed over 20 seconds) and a high bed depth (Bed depth 3, consisting of 1500g material fed over 10 seconds).

The moisture content of the feed coal was controlled to be at air-dried level, 5% per mass moisture and 10% per mass moisture. This was done to study the effect of excess moisture on the separability of the coal particles on the screen. The target moisture content of the coal was achieved by adding calculated amounts of water to the feed coal, and thoroughly mixing the coal prior to feeding it onto the screen.

The ceramic pre-drying experiments required an additional preparation step. The target amount of ceramic adsorbents, determined by the required ceramics-to-coal mass ratio, was weighed off and added to the already moisture-controlled feed coal, upon which it was thoroughly mixed prior to feeding the screen. A timer was used to start feeding the screen once the initial target contact time of 30s (and later a target of 120s) had been reached.

Another variable that was controlled was the bed depth on the screen during operation. The bed depth was controlled by the mass material fed onto the screen over a fixed time. The bed depths were a low bed depth (Bed depth 1, consisting of 500g material fed over 20 seconds), a medium bed depth (Bed depth 2, consisting of 1500g material fed over 20 seconds) and a high bed depth (Bed depth 3, consisting of 1500g material fed over 10 seconds). Figure 3.5a-c shows photos of the three bed depths taken during operation.

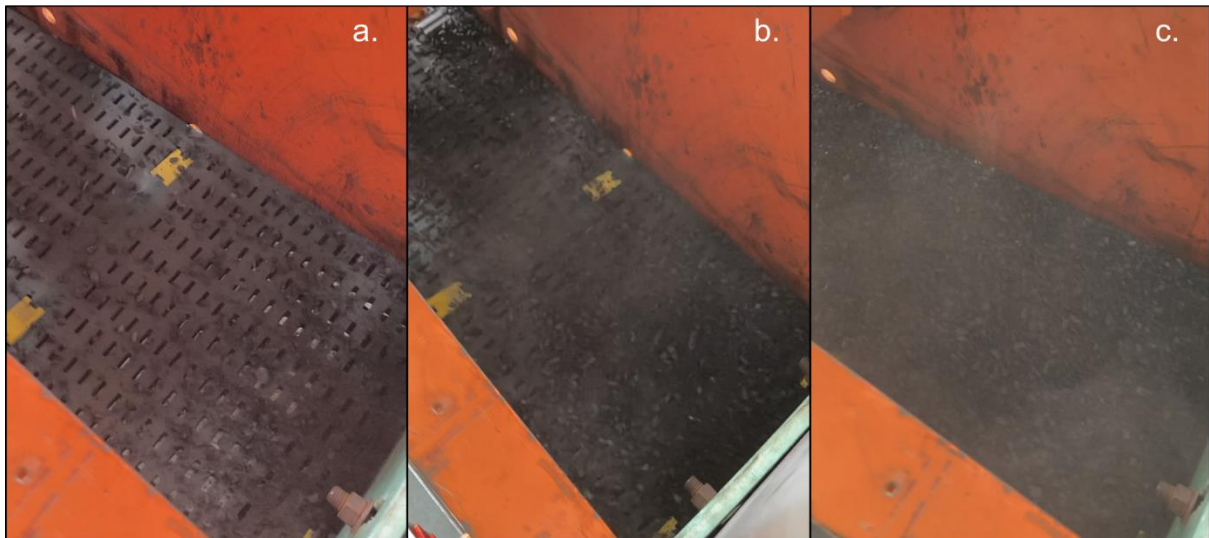


Figure 3.5: Bed depths during operation a) Bed depth 1 b) Bed depth 2 c) Bed depth 3

Three conditions were tested, namely normal operation, operation where the airflow had been switched on, and operation where the feed coal had been mixed with the ceramic spheres for 30 seconds (and later 120 seconds) prior to feeding the screen

3.3.3 Analyses

For each individual run, both the undersize and oversize particles were collected. The collected samples were then analysed for particle size distribution and moisture content. The moisture content was taken according to the SANS 5924:2009 standard. The oven used is shown in Figure 3.6a.

The particle size distribution analysis was done after the moisture analysis, and according to the ASTM D4749 standard. The laboratory sieves and sieve shaker used are shown in Figure 3.6b.



Figure 3.6: Photographs of a) the oven used and b) the sieve shaker used

3.4 Calculations

The percentage surface moisture present in the undersize and oversize particles was calculated using the weight before drying and weight after drying, and applying equation 3.1.

$$M_{wt\%} = \frac{(M_B - M_A)}{M_A} \quad 3.1$$

Where:

$M_{wt\%}$ = Moisture as weight percentage

M_B = Mass of sample before drying

M_A = Mass of sample after drying

The particle size distribution data collected from the analyses was used to calculate the feed PSD (particle size distribution). This was done by adding the weight per particle size range of the undersize and oversize particles using equation 3.2.

$$M_{f,x} = M_{u,x} + M_{o,x} \quad 3.2$$

Where:

$M_{f,x}$ = Mass of feed for particles with size range x

$M_{u,x}$ = Mass of particles in size range x collected as undersize

$M_{o,x}$ = Mass of particles in size range x collected as oversize

The undersize efficiency was then calculated using equation 3.3.

$$\%U_{eff} = \frac{M_{u,u}}{M_{u,f}} \times 100 \quad 3.3$$

Where:

$\%U_{eff}$ = Undersize efficiency as percentage

$M_{u,u}$ = Mass of undersize particles in undersize

$M_{u,f}$ = Mass of undersize particles in feed

The undersize efficiency per particle size range was then calculated using equation 3.4.

$$\%U_{eff,x} = \frac{M_{u,x}}{M_{f,x}} \times 100 \quad 3.4$$

Where:

$\%U_{eff,x}$ = Undersize efficiency as percentage for particle size range x

$M_{u,x}$ = Mass of undersize particles in undersize for particle size range x

$M_{f,x}$ = Mass of undersize particles in feed for particle size range x

CHAPTER 4: RESULTS

The results obtained during this study were compared to a basis dry screening experiment repeated with different aperture size panels. The basis experiment is discussed, upon which the influence of free moisture and bed depth on dry screening is discussed. This is repeated using both 5.6 mm and 2.8 mm aperture size panels. The influence of adding airflow is discussed, followed by the influence of the ceramic pre-drying.

4.1 Dry screening of small coal particles

4.1.1.1 Basis for screening efficiency when using 5.6 mm aperture size panels

To determine a basis for the efficiency of the screen, it was operated with 5.6 mm aperture panels and the standard coal feed at inherent moisture and at -6.7 mm to +0.5 mm size range as explained in Section 3.3.1. Figure 4.1 shows the undersize efficiency obtained from this screen for three different repetitions.

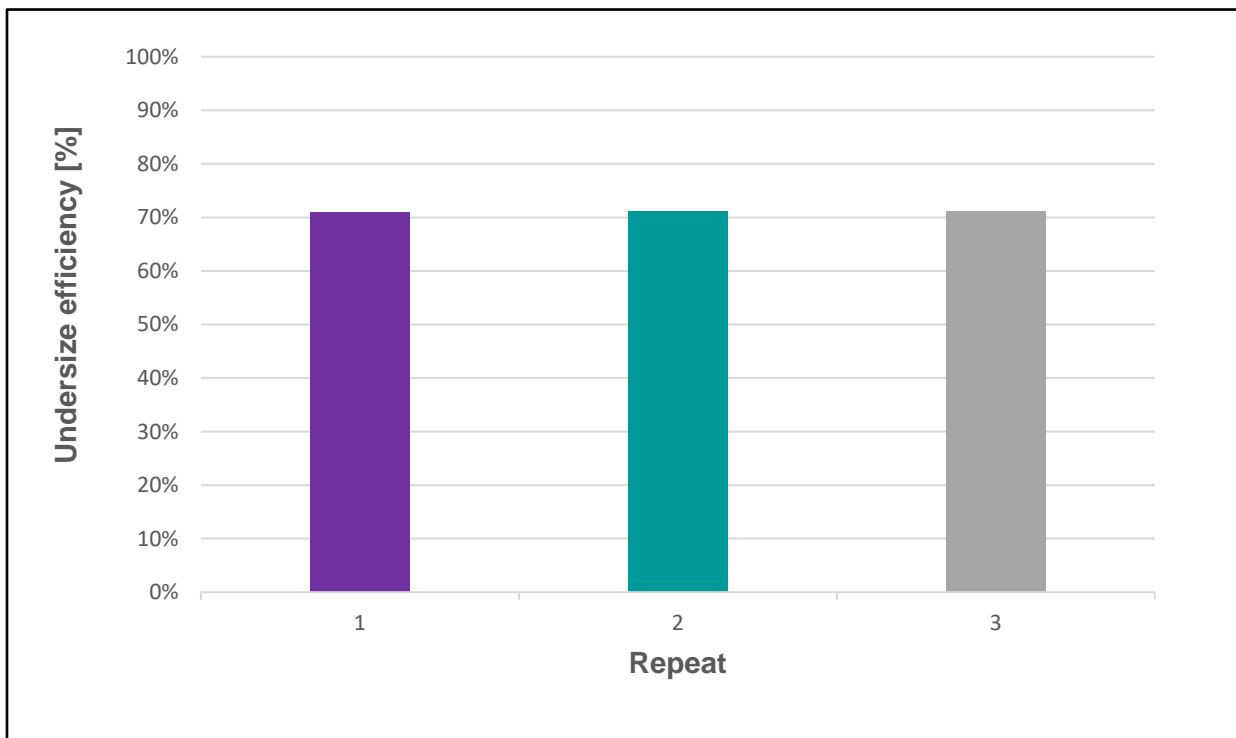


Figure 4.1: Undersize efficiencies for basis dry screening using 5.6 mm aperture size panels

Figure 4.1 shows that an average undersize efficiency of 71% across all particle size ranges was obtainable under the aforementioned operating conditions. The apparatus proved to be reliable by giving a 95% confidence interval of 0.07%. This efficiency represents the best possible performance of the screen under set conditions and was used to compare the screen's performance when other variables were introduced.

4.1.1.2 Basis for screening efficiency using 2.8 mm aperture size panels

When using the 2.8 mm aperture screen panels with the same pure coal feed, the undersize efficiency across all particles size ranges and bed depths was calculated to be 48%, with a 95% confidence interval of 0.56%. The results of the three repetitions are shown in Figure 4.2.

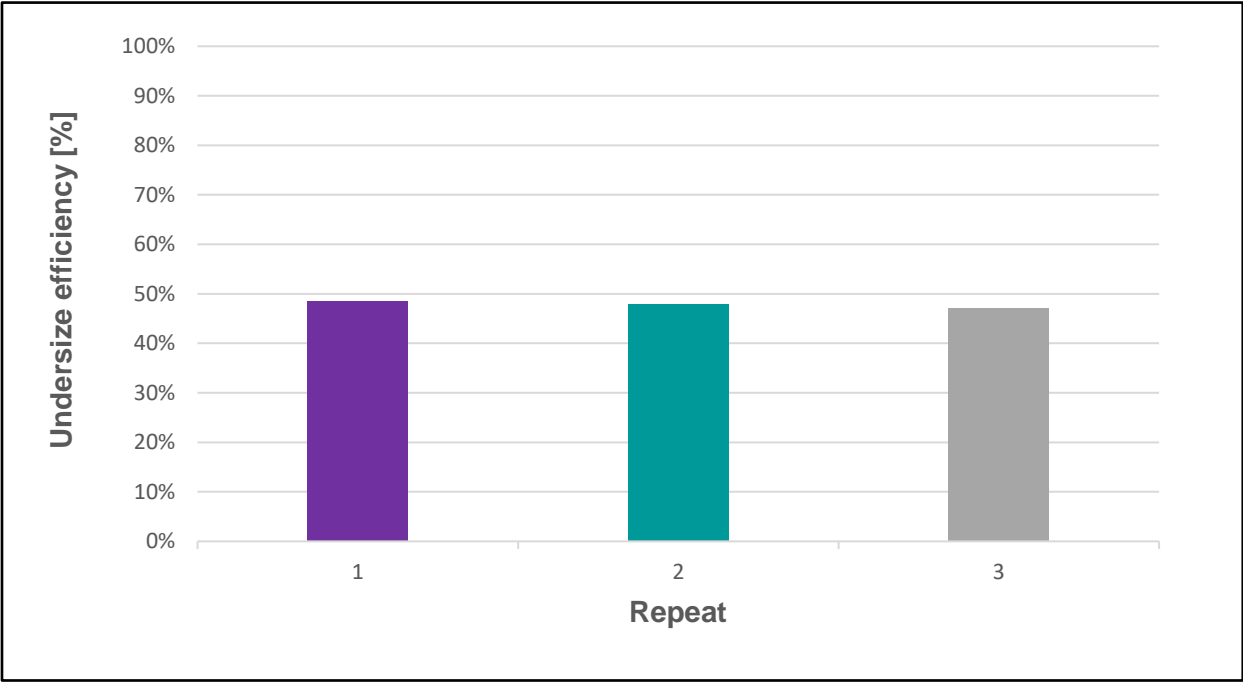


Figure 4.2: Undersize efficiencies for basis dry screening using 2.8 mm aperture size panels

The expected decrease in efficiency from Figure 4.1 to Figure 4.2 is caused by the increased number of near-size particles relative to the total amount of undersize particles. Looking at the probability formula as shown in Section 2.3.2 (Pelevin, 2020:1), it can be derived that the closer the particle diameter divided by the aperture size of the sieve is to 1, the smaller the probability of the particle passing the screen. It can thus be concluded that near-size particles are less likely to pass through the screen.

4.1.2 Influence of moisture

4.1.2.1 Influence of moisture when using 5.6 mm aperture size panels

To determine the influence of moisture on the screening performance, the moisture content of the feed coal was varied, as described in Section 3.3.2, and compared with the efficiency of the screen when fed with coal at inherent moisture content. This is shown in the graph in Figure 4.3.

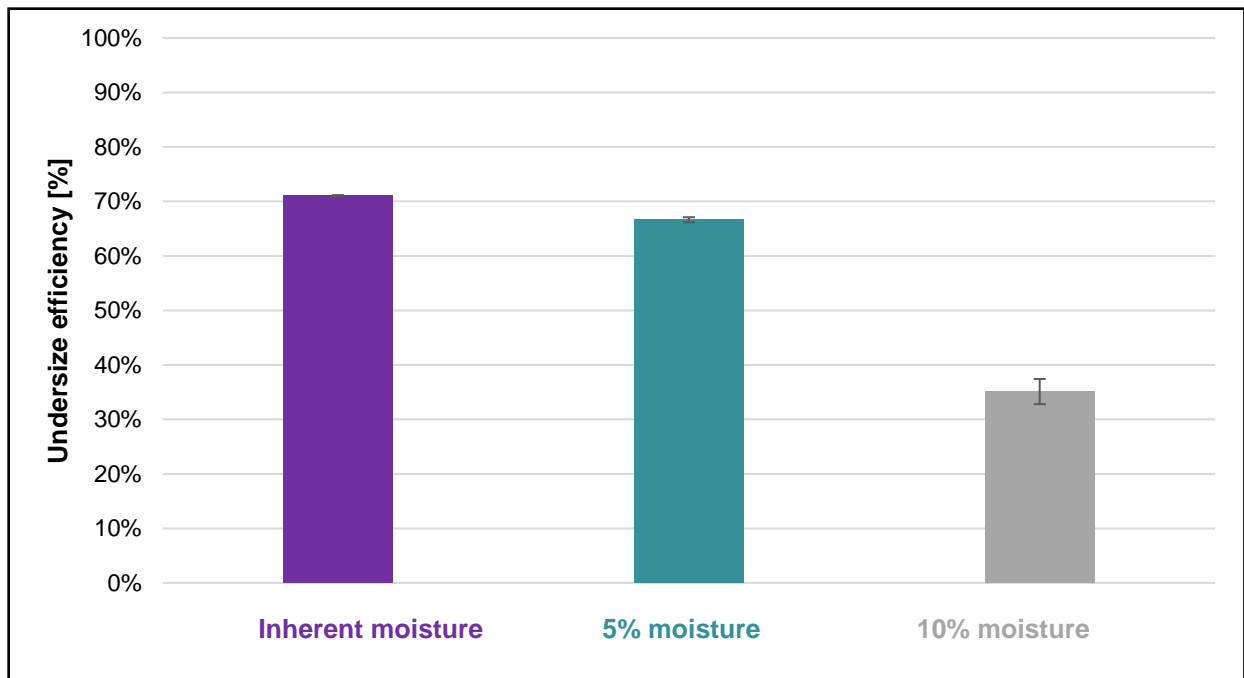


Figure 4.3: Undersize efficiencies when screening the standard feed with varying moisture contents using 5.6 mm aperture size panels

The graph in Figure 4.3 indicates that an increase of surface moisture content to 5% per weight did not significantly affect the screenability of the coal, since it only showed a small deviation from the basis undersize screening efficiency. At this moisture level, the particles were still free to move in relation to each other. This allowed each particle to present to the surface of the screen, giving it a high probability of passing through. An increase to 10% coal feed moisture content proved detrimental to screening efficiency. Research by Diedericks *et al.*, (2020:3) reported that, for coal, a moisture content above 5% by weight has a negative influence on the processing and handleability thereof. The reason for this is two-fold: a) the agglomeration and formation of pseudo larger coal particles decrease the probability of the particles passing along the length of the screen, leading to more particles reporting to the overflow, and b) particles adhere to the surfaces of the screen and panels instead of moving to the screen openings. This was especially true for the finer particle sizes and was proven by an efficiency analysis for each particle size, as shown

in Figure 4.4. This figure reports the results for a medium bed depth. For other bed depths, which yielded similar results, please refer to Appendix 6.A.

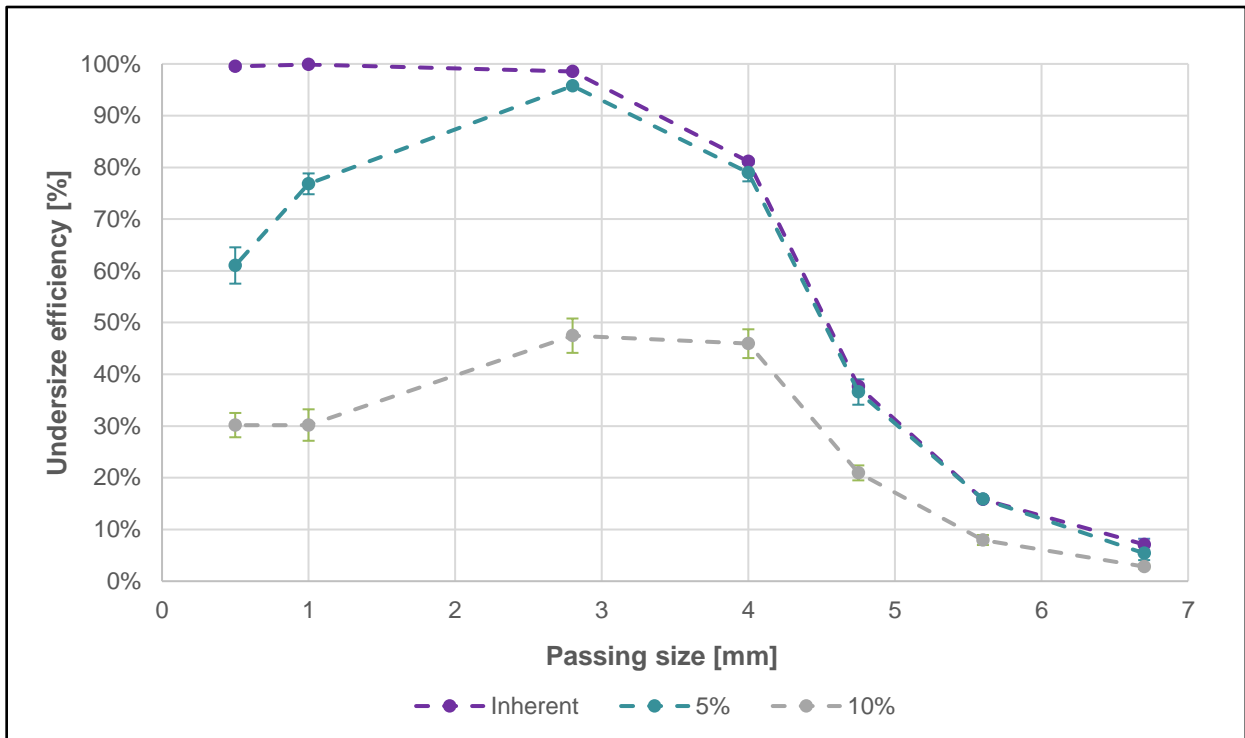


Figure 4.4: Efficiency analysis for each particle size range for basis screening with varying moisture contents using a 5.6 mm aperture size panel

Figure 4.4 illustrates that the behaviour of the 5% moisture content by weight feed coal and the inherent moisture content feed coal was the same for particles above 2.8 mm. Particles smaller than 2.8 mm showed a decline in efficiency. For the smaller particle sizes, the adhesion forces created by the presence of free moisture were large enough to allow for agglomeration of the finer particles to the surfaces of the larger particles, causing these finer particles to report to the oversize stream. For the particles larger than 2.8 mm, the forces exerted by the screen were large enough to break the agglomerates. An increase in the surface moisture content to 10% by weight increased the adhesion forces to a point where the forces exerted on the particles by the screen were not large enough to break the surface tension, allowing larger particles to also agglomerate, and resulting in more particles reporting to the oversize stream. This significantly decreased the undersize efficiency of the screen, as indicated by the grey line in Figure 4.4. When adding the increase in carry over to the accumulation of particles on the screen panels (please refer to Figure 4.5 for a visual presentation of this phenomenon), the decrease in efficiency for the 10% moisture content by weight feed coal was much larger than the 5% moisture content by weight feed coal.



Figure 4.5: Photograph showing agglomeration of wet particles to the screen surface

4.1.2.2 Influence of moisture when using 2.8 mm aperture size panels

The negative effect of surface moisture on the efficiency of screening was exaggerated when the panel aperture was reduced to 2.8 mm. This is shown in the graph in Figure 4.6

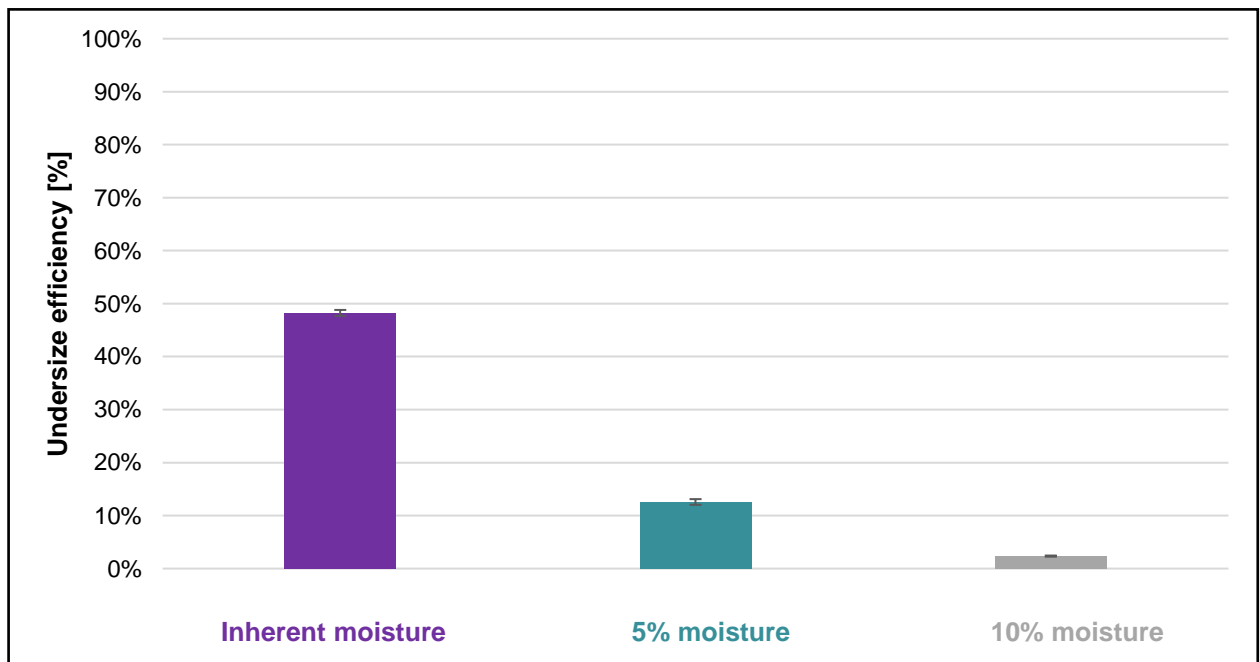


Figure 4.6: Undersize efficiencies when screening the standard feed with varying moisture contents using a 2.8 mm aperture size panel

Figure 4.6 shows an undersize efficiency decrease of nearly 36% when increasing the moisture content from inherent moisture to 5% moisture for a medium bed depth compared to screening at 5.6 mm, which performed similarly with inherent moisture and 5% moisture for a medium bed depth. It was previously determined that, at 5% moisture content, the influence of moisture is mainly on particles smaller than 2.8 mm. When screening at 2.8 mm, all undersize particles are smaller than 2.8 mm, and the influence of the moisture is thus exaggerated. This was proven by an efficiency analysis for each particle size range, as shown in Figure 4.7

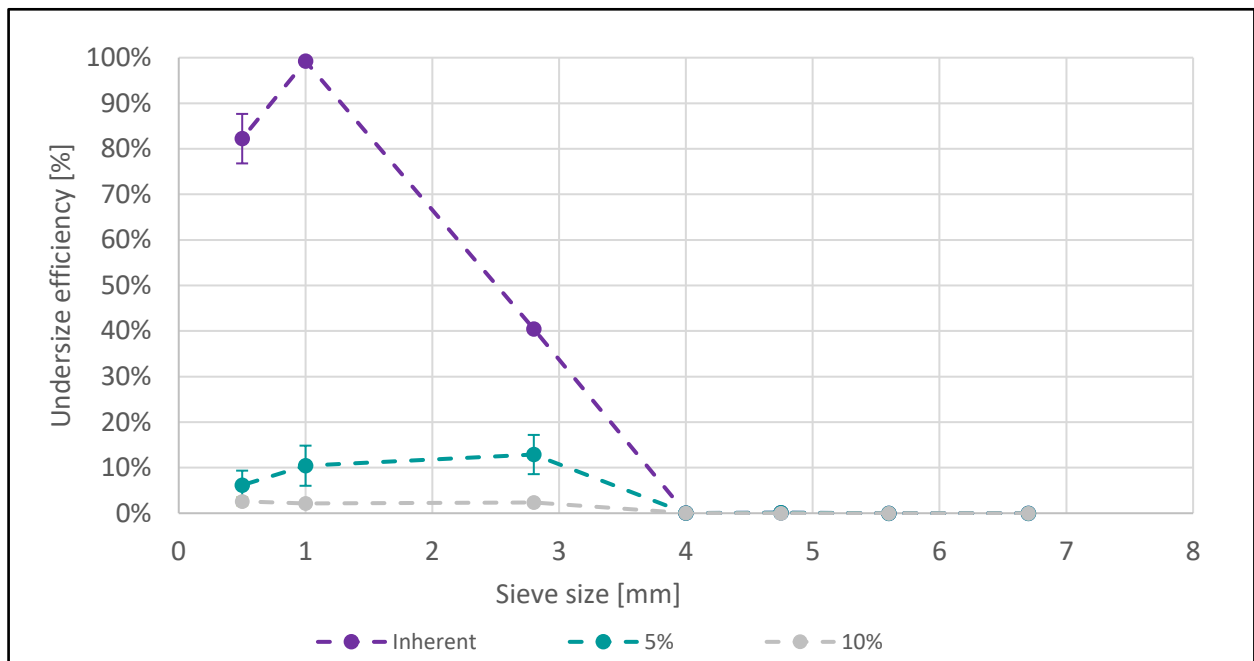


Figure 4.7: Undersize efficiency analysis for each particle size range for basis screening with varying moisture contents using a 2.8 mm aperture size panel

Figure 4.7 confirms that all undersize particles when screening at 2.8 mm are greatly affected by moisture through the mechanism of agglomeration at a medium bed depth. For other bed depths, refer to Appendix 6.B.

4.1.3 Influence of bed depth

4.1.3.1 Influence of bed depth using 5.6 mm aperture size panels

It was expected that the bed depth would have a significant influence on the performance of the screen, but for the coal fed at inherent moisture levels, the influence of bed depth was negligible, as shown in Figure 4.8.

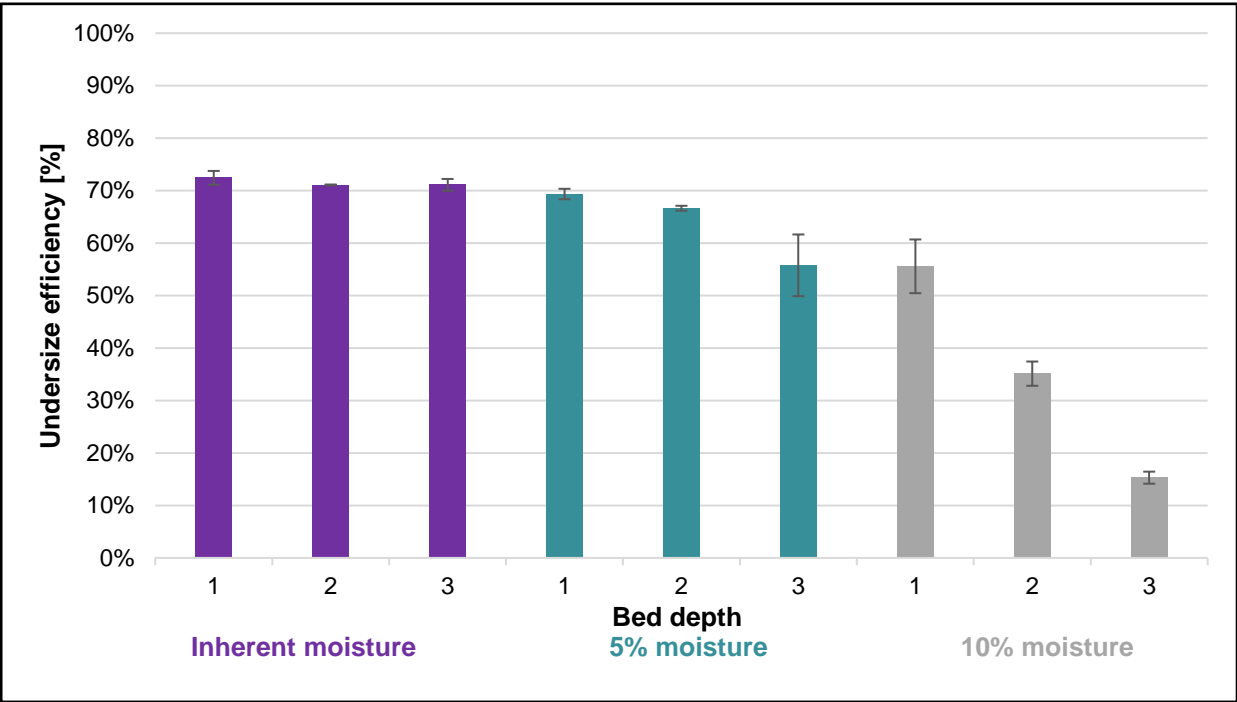


Figure 4.8: Undersize efficiencies for basis screening with varying bed depths using 5.6 mm aperture size panels

As seen in Figure 4.8, the effect of bed depth was exaggerated with an increase in moisture content when using a 5.6 mm aperture size. This could be explained by the increased interaction of particles due to the deeper bed depths resulting in increased agglomeration of particles, which reduced the stratification that took place. The reduced stratification became more evident at deeper bed depths as particles no longer reached the screen surface, reducing the probability of each particle to pass the screen.

Figure 4.9 illustrates the efficiency analysis for each particle size range showing the influence of bed depth on all the particles.

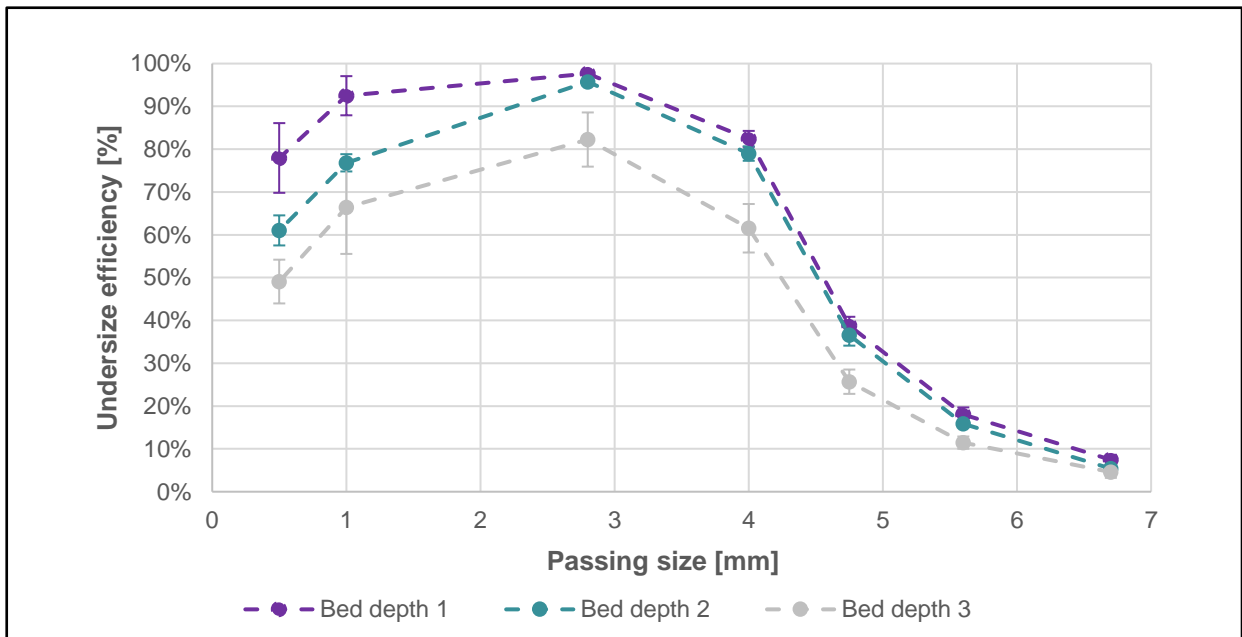


Figure 4.9: Efficiency analysis for each particle size range with varying bed depth using 5.6 mm aperture size panels and 5% moisture content

In Figure 4.9 it can be seen that the additional particles on the bed reduce the undersize efficiency by causing more undersize particles to agglomerate to oversize particles and report as carried-over particles to the overflow stream. This was especially true for the deepest bed depth where the smaller particles had to move to the bottom of the bed via stratification to present to the screen surface. The same applied to the 10% moisture content by weight as shown by the efficiency analysis for each particle size range shown in Figure 4.10.

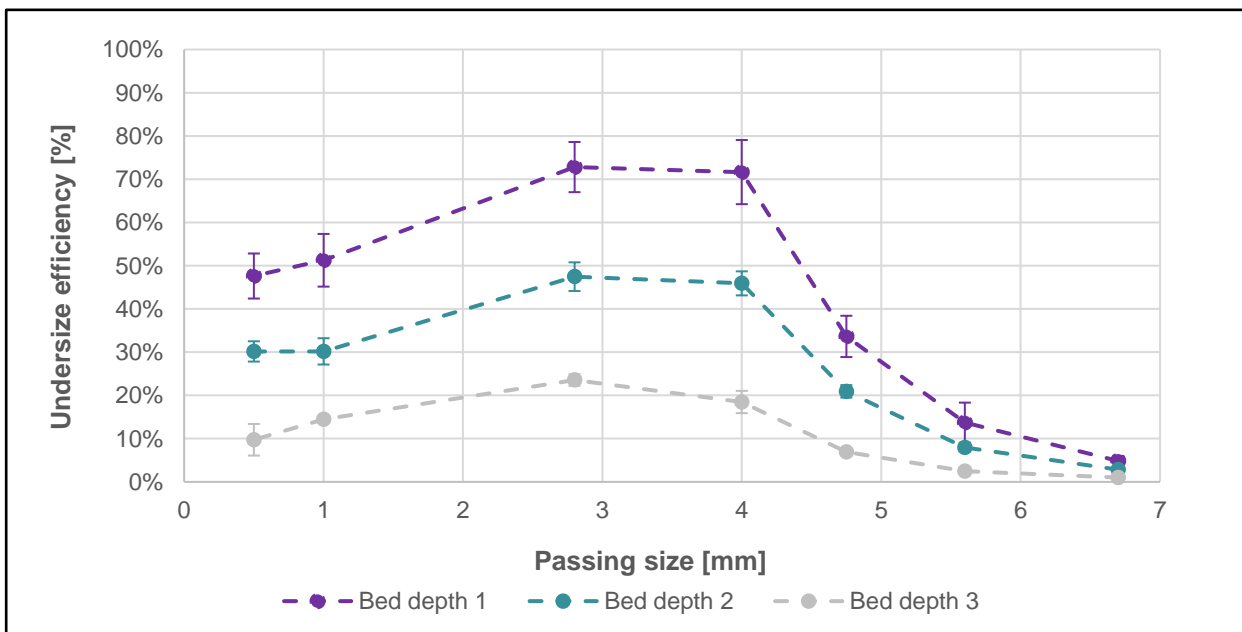


Figure 4.10: Efficiency analysis for each particle size range with varying bed depth using 5.6 mm aperture panels at 10% moisture content

Figure 4.10 confirms that the effect of bed depth is exaggerated with increasing moisture. This is demonstrated by the large difference in undersize efficiencies for each particle size range, which is again caused by the agglomeration of particles, resulting in reduced stratification and a lower probability for each particle to pass the screen surface.

4.1.3.2 Influence of bed depth when using 2.8 mm aperture size panels

The effect of bed depth when screening with 2.8 mm aperture panels is shown in the graph in Figure 4.11.

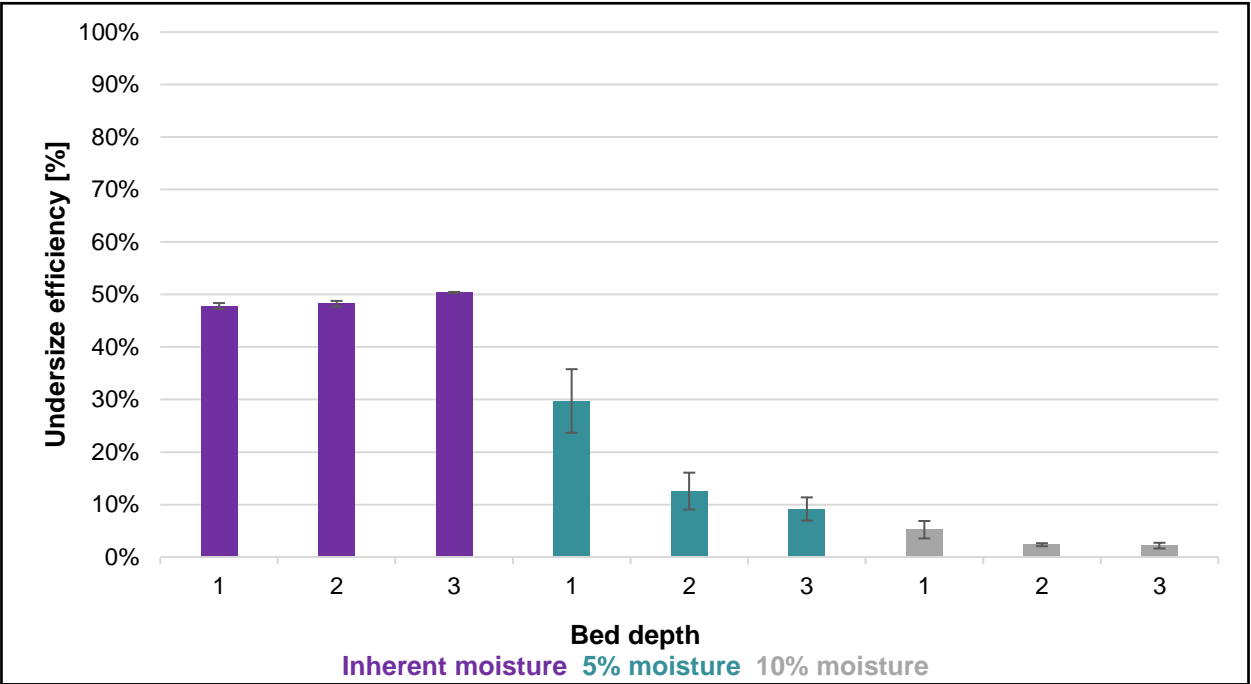


Figure 4.11: Undersize efficiencies for varying bed depths and moisture using 2.8 mm aperture size panels

The graph in Figure 4.11 confirms that, when using a 2.8 mm screen, the efficiency becomes greatly reduced and the influence of bed depth is exaggerated at 5% moisture content by weight, since all particles are now smaller than 2.8 mm and affected by moisture. The effect of 10% moisture content by weight is so significant on the smaller particles that almost no screening takes place, eliminating the effect of bed depth.

The efficiency analysis for each particle size range is only done for the 5% moisture content screening, as shown in Figure 4.12.

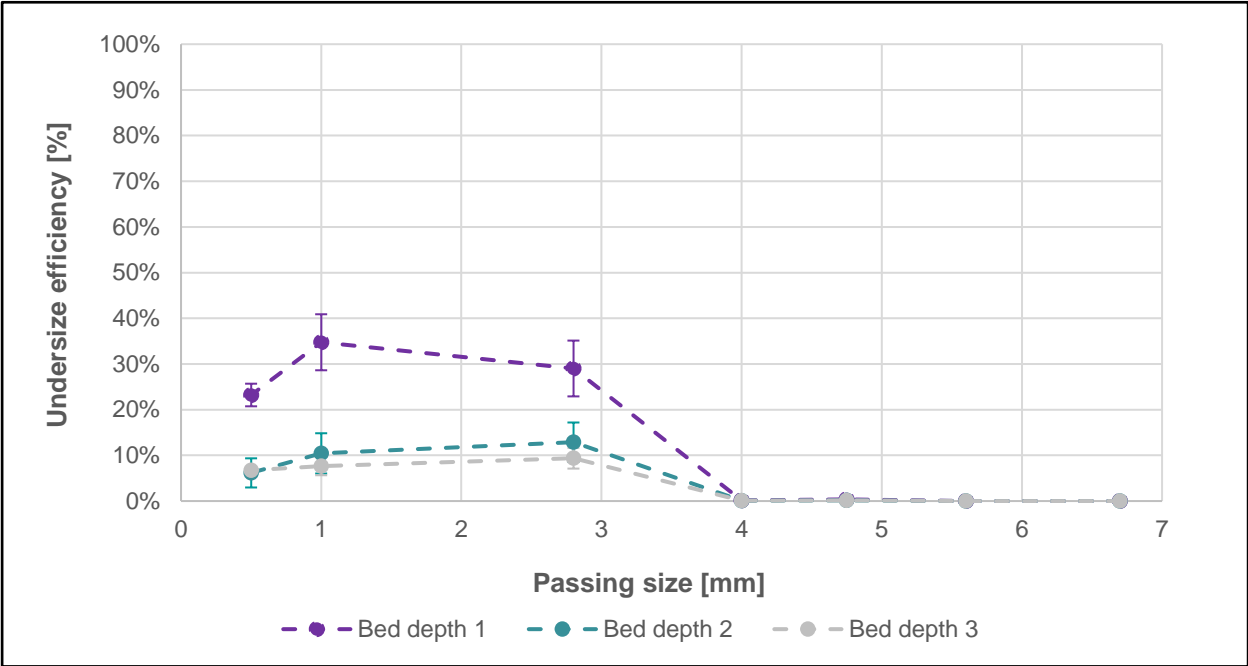


Figure 4.12: Efficiency analysis for each particle size range with varying bed depth using 2.8 mm aperture size panels at 5% moisture content

Figure 4.12 shows a reduction of undersize efficiency at 5% moisture content by weight for the - 1 mm + 0.5 mm particle size range from 99% with inherent moisture content to 35% for a low-bed depth and 10% for a medium-bed depth. If this is compared to the 5% moisture content by weight screening with 5.6 mm aperture panels in the same size range showing a 92% undersize efficiency at a low-bed depth and 77% at a medium-bed depth, it is clear that the influence of moisture is increased with decreasing aperture size and the effect of bed depth is increased with increasing moisture content.

4.2 Dry screening with airflow

4.2.1 Effect of added airflow when using 5.6 mm aperture size panels

In general, the addition of airflow did not yield any significant improvement in the undersize screening efficiency. The short retention time of only 5 seconds did not give enough time for the added airflow to dry these particles to the point where it promoted screening. This is illustrated in Figure 4.13.

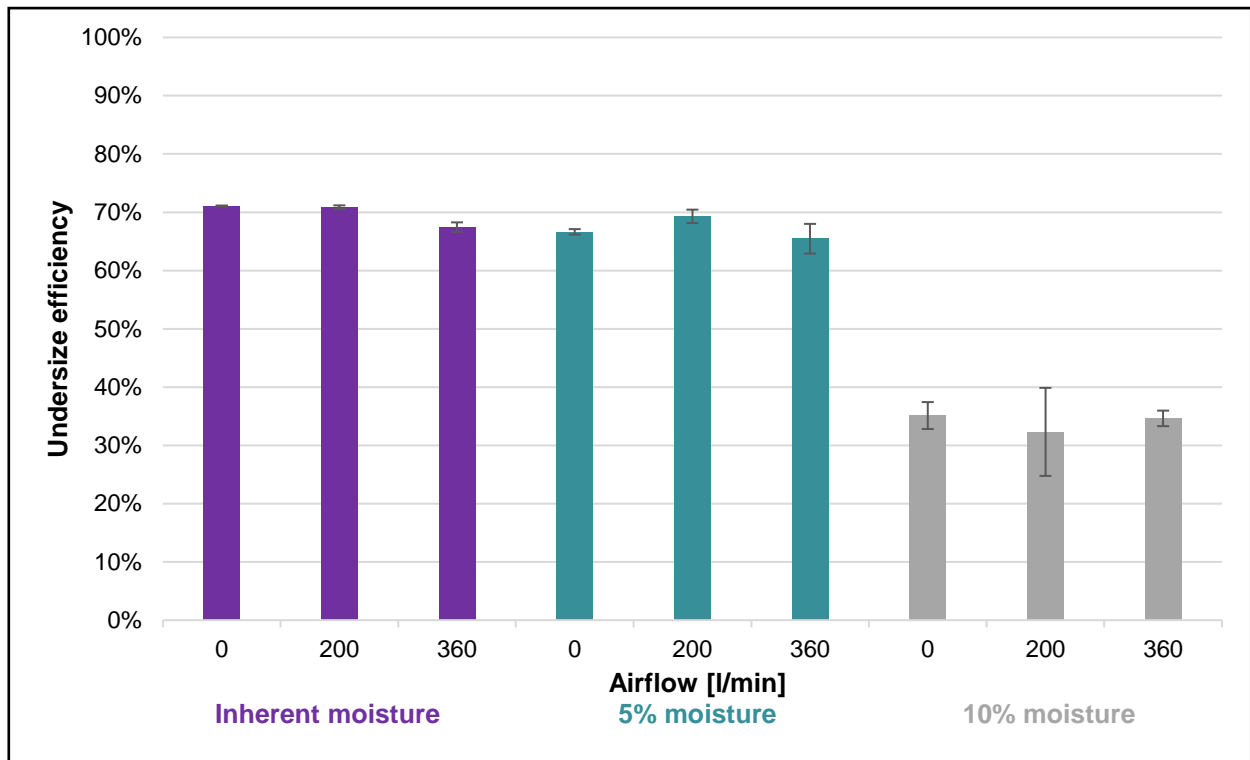


Figure 4.13: Undersize efficiencies with varying airflow rates when using 5.6 mm aperture size panels

Figure 4.13 clearly shows that the addition of airflow did not have any significant impact on the undersize efficiency. Although there is variation in the graph, specifically at 10% moisture, no specific trend can be identified and the variation falls within the experimental errors. Large errors are present due to the reduced handleability of small coal particles above 5% moisture content. The airflow did not reduce the moisture content by any significant margin. The average undersize moisture content after screening at 5% moisture content by weight was 4.92% by weight. With the addition of airflow at 200 l/min, the moisture content was 4.76%; at 360 l/min, it was 4.70%. This was also the case when screening at 10% moisture content by weight, where the average undersize moisture content after screening was 7.22% and, at best – with the addition of 360 l/min airflow – was reduced to 6.69%. This proved that the 5-second retention time was insufficient to reduce the surface moisture. The study by Van Rensburg (2019:80) used airflow to efficiently dry fine coal, but required retention times between 10 and 20 minutes.

4.2.2 Effect of added airflow when using 2.8 mm aperture size panels

The addition of airflow again had no significant impact when screening at 2.8 mm as shown in Figure 4.14.

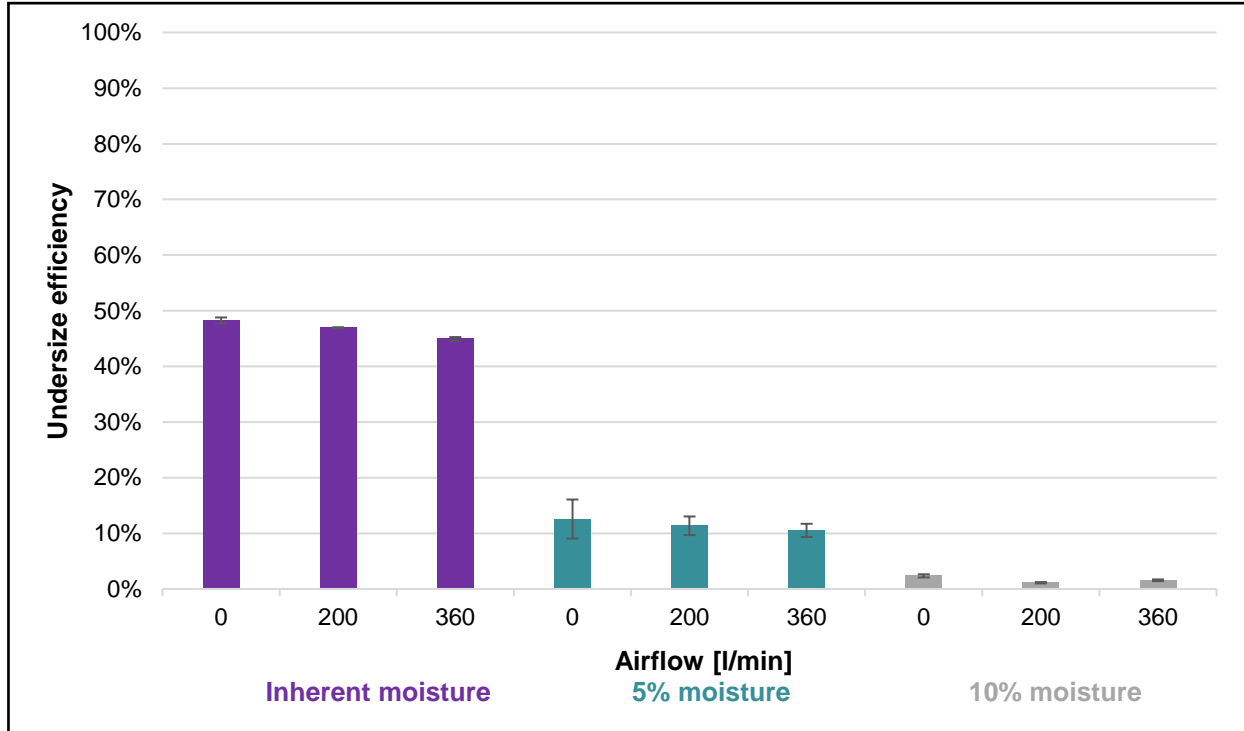


Figure 4.14: Undersize efficiencies with vary airflow rates when using 2.8 mm aperture size panels

Figure 4.14 confirms that the addition of airflow did not have a significant impact on the undersize screening efficiency of the smaller particles. When using the 2.8 mm panels and screening at 5% moisture content by weight, the average undersize moisture content was 6.71%. With the addition of 200 l/min airflow, it reduced to 6.41% and when screening with 360 l/min of airflow, to 5.92%. The average undersize moisture for the 10% moisture content screening could not be determined due to the very low screening efficiencies. The increase in undersize moisture content when using a smaller aperture size proves that smaller particles tend to retain more moisture due to the increased surface area relative to mass.

4.3 Ceramic pre-drying of coal

4.3.1 Basis for screening using the adapted feed

The new feed as described in Section 3.3.1 was used to create a new basis for efficiency. Figure 4.15 shows the efficiency analysis for each particle size range for a medium bed depth. For other bed depths, refer to Appendix 6.C.

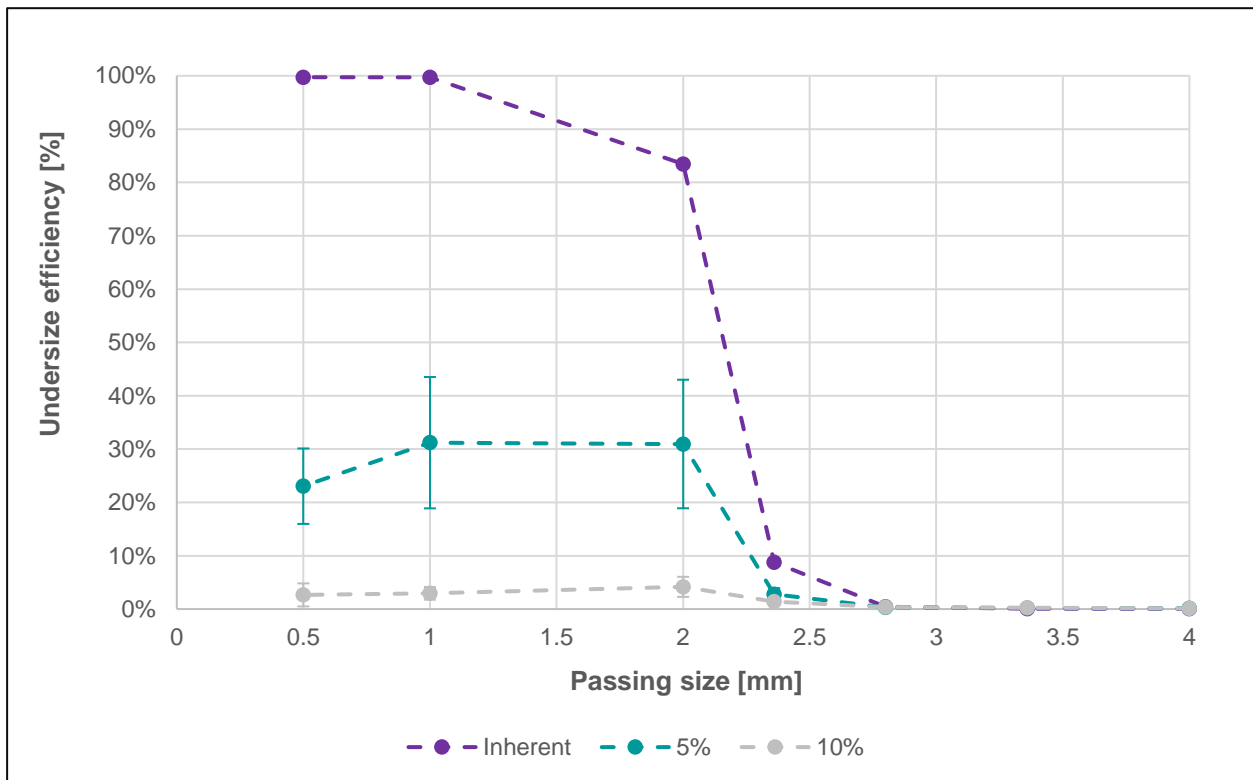


Figure 4.15: Efficiency analysis for each particle size range for basis screening of adapted feed

Compared to the original feed, it can be observed that the influence of moisture was greater on the new feed due to the larger fraction of particles smaller than 2.8 mm, resulting in more agglomeration. The undersize screening efficiency reduced from 90% at inherent moisture conditions to 31% with the addition of 5% moisture content by weight, and to as low as 2% with the addition of 10% moisture content by weight. It can therefore be concluded that the smaller the particles the more important it is to remove the moisture for efficient screening. Ceramic adsorbents have been proven to efficiently dry fine coal particles with very little contact time.

4.3.2 Influence of ceramic pre-drying

Figure 4.16 shows that the addition of ceramics prior to feeding the screen improved the performance of the 5% and 10% moisture content feed coal.

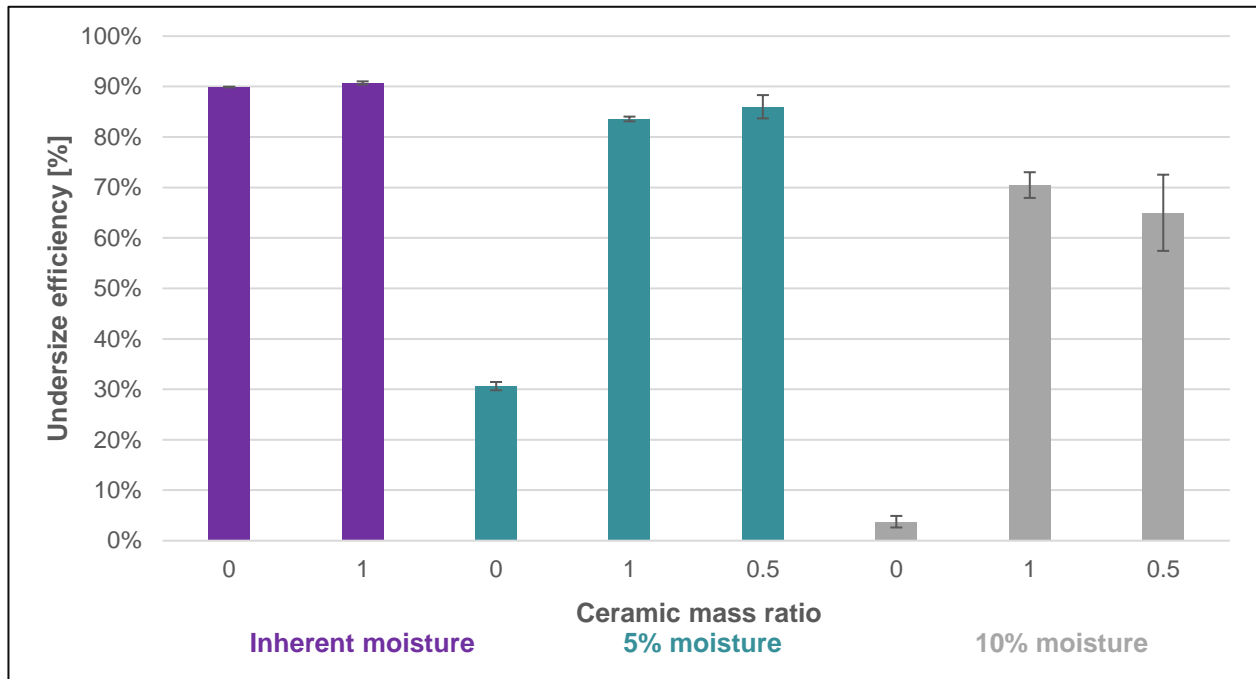


Figure 4.16: Undersize efficiencies with addition of ceramics in different mass ratios

The graph in Figure 4.16 shows an increase from 30% when screening at 5% moisture content by weight to above 80% with the addition of ceramics. This can be ascribed to the efficient moisture reduction by the ceramic adsorbents with only 30 seconds of contact time. The average moisture content of the undersize particles after screening reduced from 5.80% when screening at 5% moisture content, to 4.35% with the addition of ceramics in a 1:1 ceramic to coal mass ratio, and to 4.41% with a 0.5:1 ceramic to coal mass ratio. When screening at 10% moisture content by weight, the average undersize moisture content after screening reduced from 7.06% to 5.36% using a 1:1 ceramic to coal mass ratio, and to 5.83% using a 0.5:1 ceramic to coal mass ratio. The reduction in moisture content prior to and during screening and the effect thereof on undersize screening efficiency is better quantified by an efficiency analysis on each particle size range.

The graph in Figure 4.17 shows the efficiency analysis for each particle size range.

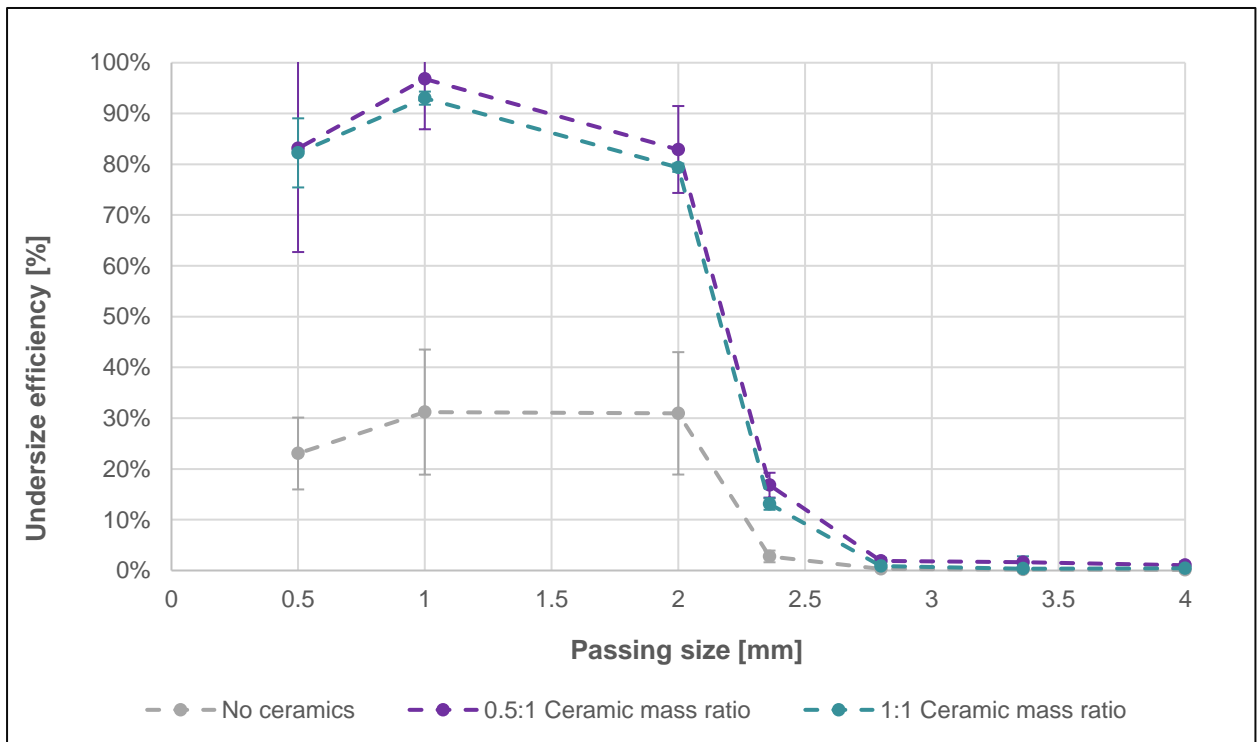


Figure 4.17: Efficiency analysis for each particle size range with the addition of ceramic adsorbents when screening at 5% moisture content

The influence of the added ceramics on the different particle sizes for a medium bed depth are shown in Figure 4.17 for the 5% moisture content by weight coal feed. Refer to Appendix 6.D for the low and high bed depths. The ceramics were able to dry the 1 mm passing particles more rapidly than the 0.5 mm passing particles. This is mainly attributed to the larger cumulative surface area of the smaller particles, which attracts more moisture than the larger particles. It is clear from the graph that the 1:1 and 0.5:1 ceramic to coal mass ratios performed similarly, indicating that the reduction of moisture content is not limited by the ceramic's capacity or available surface area, but by contact time. Therefore, a longer contact time prior to feeding will result in even better screening efficiencies, as the moisture content is still high enough to cause agglomeration in the particles smaller than 1 mm.

This was more evident when screening at 10% moisture content by weight. The efficiency analysis for each particle size range when screening with ceramics at 10% moisture content by weight, is shown in Figure 4.18.

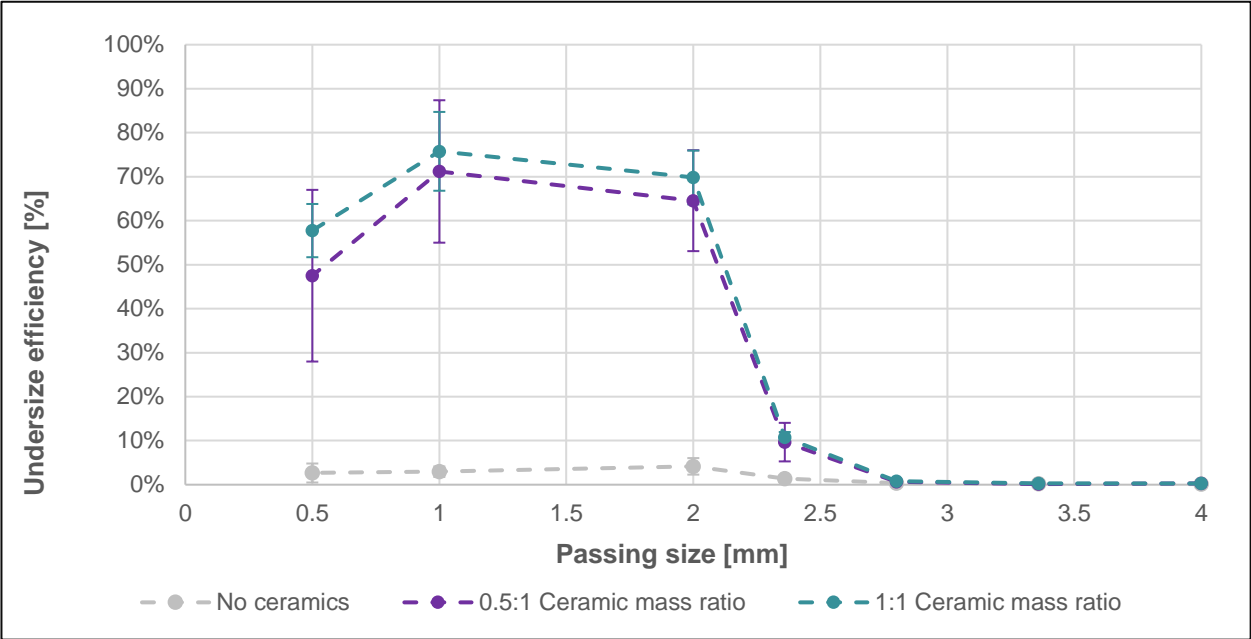


Figure 4.18: Efficiency analysis for each particle size range with the addition of ceramic adsorbents when screening at 10% moisture content

The influence of the added ceramics on the different particle sizes for a medium bed depth are shown in Figure 4.18 for the 10% moisture content by weight coal feed. Refer to Appendix 6.E for the low and high bed depths. Again, it is clear that the ceramics were able to dry the 1 mm passing particles more rapidly than the 0.5 mm passing particles, due to the larger relative surface area of the smaller particles attracting more moisture. As mentioned above, the ceramics did not reduce the average undersize moisture content to below 5% after screening, and agglomeration took place in all the size ranges of the undersize particles, resulting in a lower than desired undersize screening efficiency. The two different mass ratios performed similarly, indicating that the reduction in moisture is not limited by the capacity of the ceramics or the surface area available for contact, but by contact time. Once more, it can be concluded that an increased contact time should result in improved efficiencies.

4.3.3 Influence of bed depth

As expected, Figure 4.19 shows that the influence of bed depth is eliminated with the 1:1 ceramic-to-coal mass ratio feed because of the rapid removal of moisture.

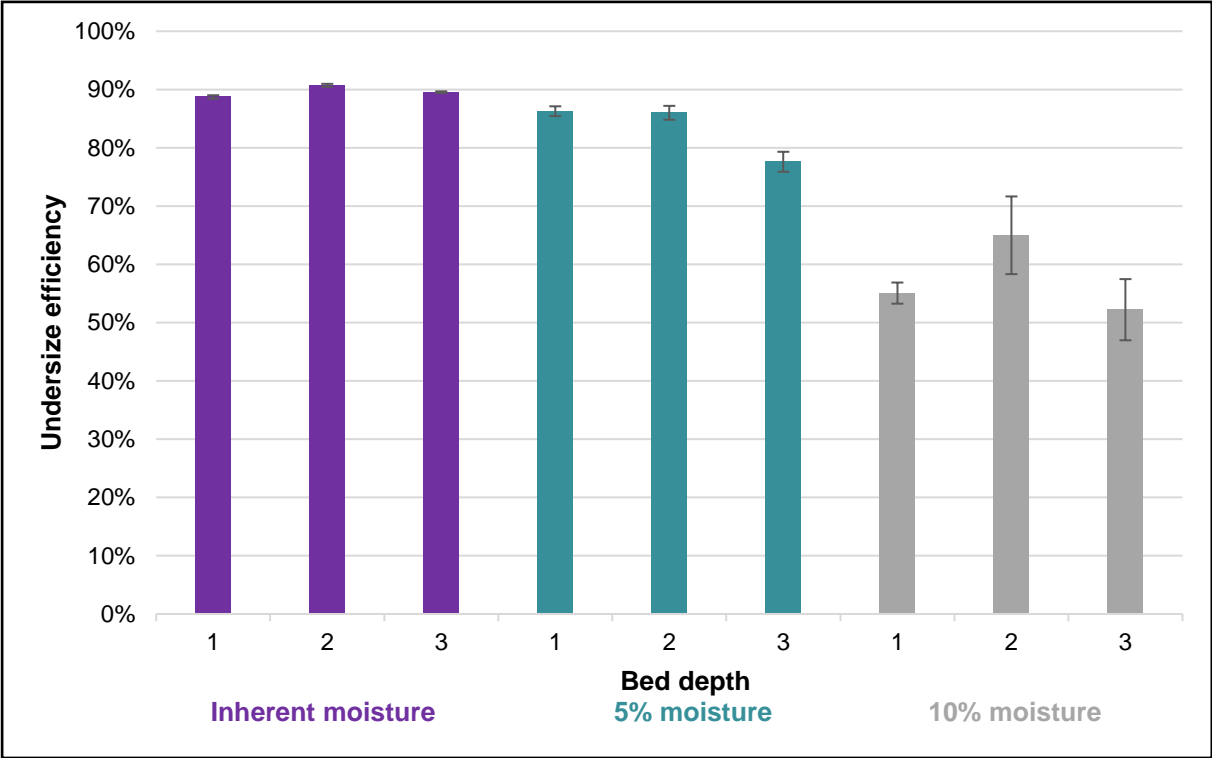


Figure 4.19: Undersize efficiencies with varying bed depths with the addition of a 1:1 ceramic to coal mass ratio

Although the graph in Figure 4.19 shows some form of variance, no specific trend showing the significantly reduced effect of bed depth could be identified. As mentioned before, the presence of moisture at contents above 5% greatly affects the handelability of coal; hence, large experimental errors are present when screening at moisture contents above 10% by weight. When screening at 5% moisture content by weight, the average undersize moisture content is reduced to below 5% and the experimental errors are much smaller. At the high bed depth, a small reduction in undersize efficiency can be identified. This is caused by the increased interaction of particles, due to the deeper bed depth. The deeper bed depth requires more stratification to take place for smaller particles to reach the screen surface, increasing the probability of particles to agglomerate and therefore reducing the probability of particles to pass the screen. As determined in Section 4.3.2, the ceramic-to-coal mass ratio can be reduced to 0.5:1 without affecting the performance, as the reduction is limited by contact time.

The 0.5:1 ceramic-to-coal mass ratio performed similarly as shown in Figure 4.20.



Figure 4.20: Undersize efficiencies with varying bed depths with the addition of a 0.5:1 ceramic to coal ratio

Figure 4.20 confirms that, at a lower ceramic-to-coal mass ratio, the effect of bed depth is still significantly reduced. Therefore, it can be concluded that the screen can be fed at a much higher capacity if the moisture is sufficiently reduced. At 5% moisture content by weight, the reduction in moisture was sufficient with 30 seconds of contact time – which was determined to be the limiting factor – but at 10% moisture content by weight, this was not the case. An increase in contact time for the 10% moisture content screening should thus improve undersize screening efficiency.

4.3.4 Influence of contact time

The initial 30 seconds of contact time was shown to adequately dry the 5% moisture coal particles for both the 1:1 and the 0.5:1 ceramic-to-coal mass ratio. The 10% moisture content coal was however not adequately dried in 30 seconds, so the contact time was increased to 120 seconds. Figure 4.21 shows the undersize efficiencies at different contact times.

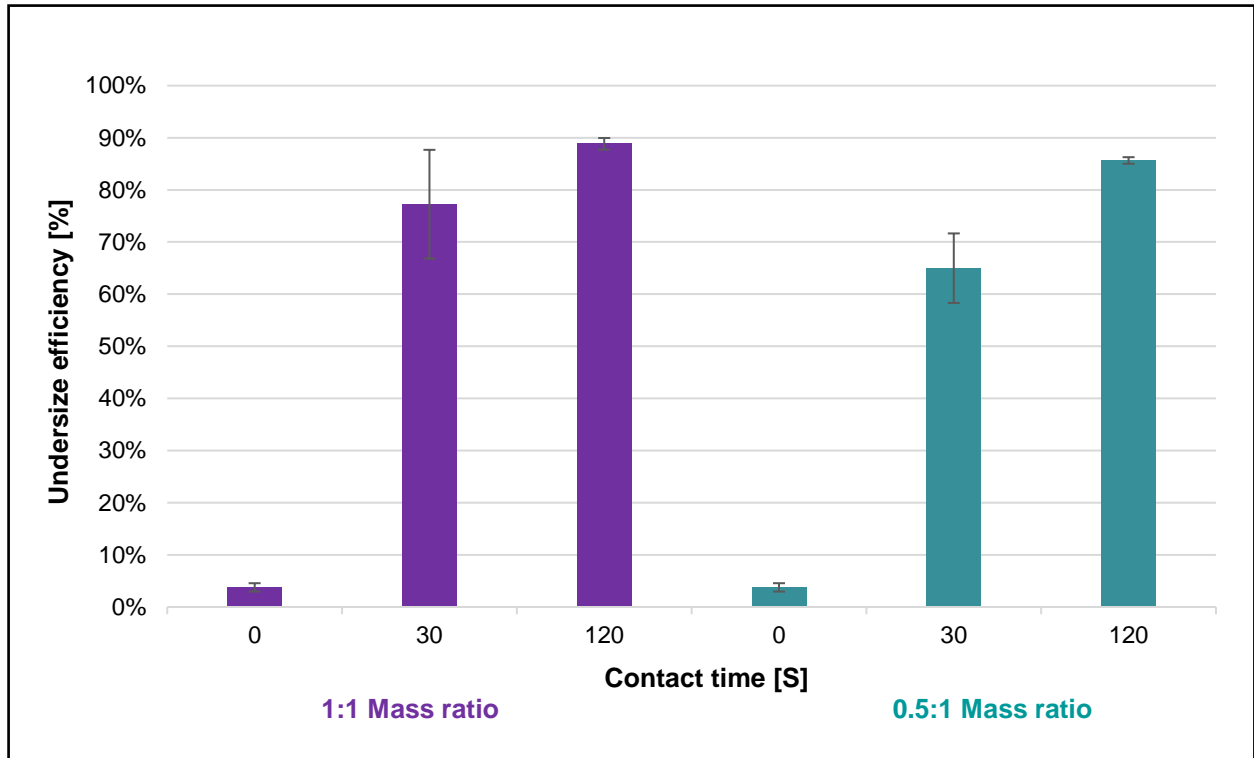


Figure 4.21: Undersize efficiencies with varying contact times and ceramic to coal mass ratios

From Figure 4.21 it can be seen that the increased contact time did increase screening efficiency, which – as stated in Section 4.3.2 – confirmed that the ceramic drying was not limited by the capacity of the ceramics or the surface area available for contact, but by contact time. When screening at 5% moisture content by weight, the average undersize moisture content after screening was reduced from 7.06% to 2.09% for a 1:1 ceramic-to-coal mass ratio, and to 2.78% for a 0.5:1 ceramic-to-coal mass ratio. Again, an efficiency analysis for each particle size range should aid in a better quantification of the results.

Figure 4.22 shows the efficiency analysis per particle size range.

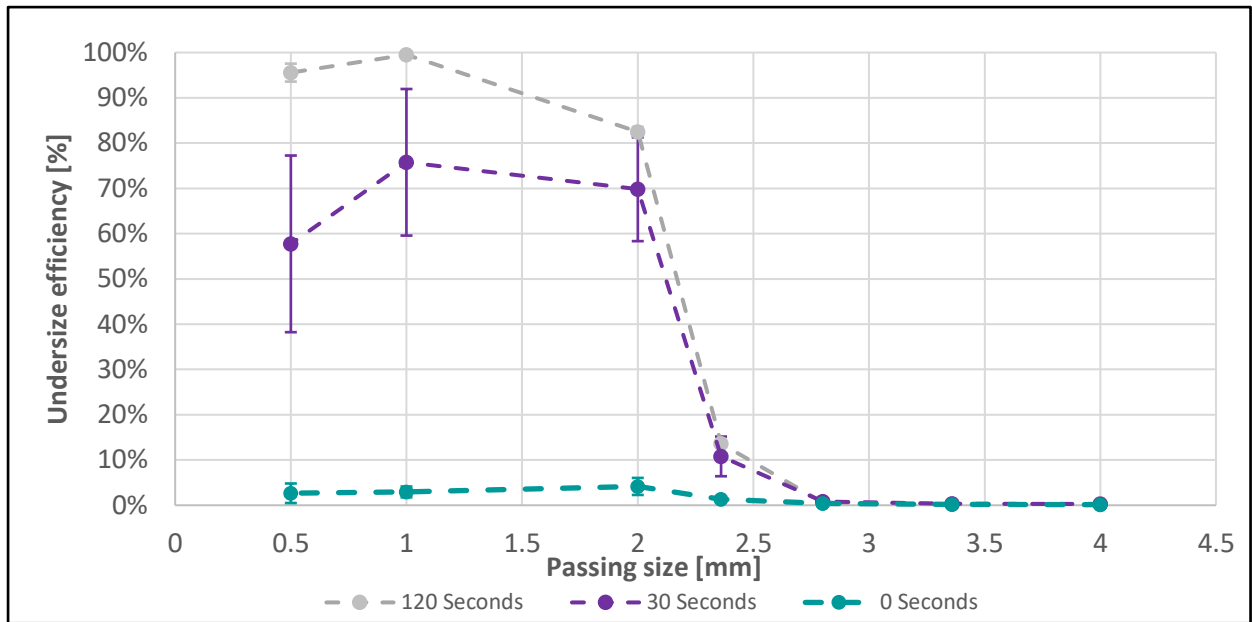


Figure 4.22: Efficiency analysis for each particle size range for varying contact times using a 1:1 ceramic-to-coal mass ratio

Figure 4.22 shows that, with 120 seconds of contact time and a 1:1 ceramic-to-coal mass ratio, the undersize efficiency of all particle size ranges are similar to screening at inherent moisture content. The average undersize efficiency was reduced to below the inherent moisture content as determined in Section 3.1.1 to be 2.58% for particles in the -4 mm + 2 mm range and 2.55% for particles in the -2 mm + 0.5 mm range. Figure 4.23 shows the same for a 0.5:1 ceramic-to-coal mass ratio.

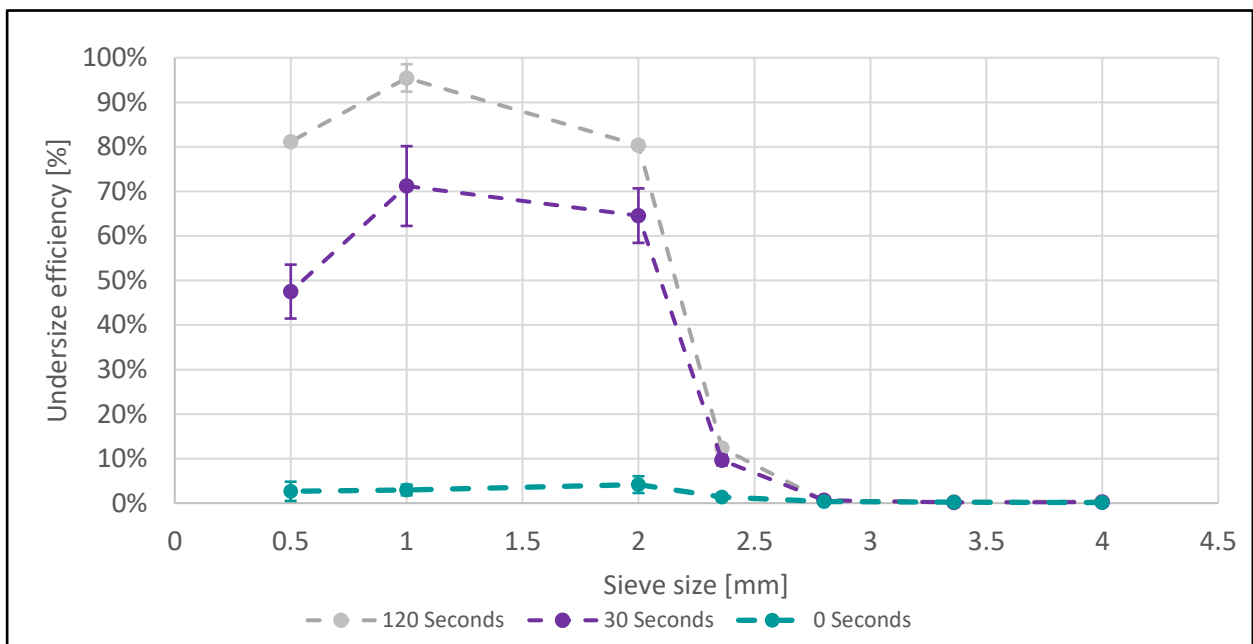


Figure 4.23: Efficiency analysis for each particle size range for varying contact times using a 0.5:1 ceramic-to-coal mass ratio

In Figure 4.23 it can be seen that agglomeration was taking place for particles in the -1 mm to + 0.5 mm range. The average undersize moisture content after screening reduced from 7.06% to 2.78% with 120 seconds of contact time at a 0.5:1 ceramic-to-coal mass ratio, which is still above the inherent moisture content and therefore confirms that there was still free moisture present, which caused the agglomeration of the small particles.

4.3.5 Concluding remarks

The results showed that free moisture content has the largest impact on dry screening efficiency. The impact of bed depth is exaggerated with the presence of moisture due to the increased interaction between particles. The key to efficient dry screening is therefore the removal of all free moisture present.

The addition of airflow was not efficient for drying coal, and, as a result, did not yield any significant improvement in the undersize efficiency of screening. The addition of ceramic adsorbents proved to be efficient in removing the free moisture content of the coal. When screening at 5% moisture content by weight, a contact time of 30 seconds proved sufficient for both a 1:1 and 0.5:1 ceramic-to-coal mass ratio. However, this was not the case for 10% moisture content where the contact time had to be increased to 120 seconds for the 1:1 and 0.5:1 ceramic-to-coal mass ratios.

CHAPTER 5: CONCLUSION, RECOMMENDATION AND CONTRIBUTION

Chapter 5 provides the conclusion, recommendation and contribution of the experiments carried out in this study. The conclusions are based on the results from chapter 4 and constructed from the research objectives. The recommendations are given to guide and improve future work in the same field of study and, finally, the contributions conclude with the impact this study could have on the coal processing industry.

5.1 Conclusion

- For coal feed at inherent moisture levels, dry screening efficiencies were the highest, resulting in a maximum efficiency of 90% for a single layer bed. The absence of moisture allowed for particles to stratify and present to the screen surface for sorting. The different bed depths that were tested had minimal influence on the screening efficiency under these conditions because of the ability of individual particles to move independent of each other and make sufficient contact with the screen surface within the retention time.
- It was determined that moisture had the greatest influence on screening efficiency. For a coal feed at 5% free moisture content, all particles smaller than 2.8 mm were adversely affected by agglomeration due to free surface moisture causing surface tension forces that were stronger than the forces exerted on the particle during screening. The dry screening efficiency in some cases was reduced from 99% for particles smaller than 1 mm to as low as 60%. However, particles larger than 2.8 mm were not affected. At 10% moisture content, all coal particles in the study were affected by agglomeration, showing that the forces exerted on the particles during screening were not sufficient to break agglomerates caused by the surface tension of free moisture on the particles. The efficiency of particles smaller than 1 mm reduced from 99% to 30%, and particles between 2.8 mm and 4 mm from 98% to 47%.
- The addition of airflow during screening did not have any significant effect on the reduction of coal moisture content and therefore screening efficiency was not improved. Airflow has been proven to be effective in reducing coal moisture content, but the contact time proved too little to effectively reduce moisture content and screening efficiency.
- The use of ceramics to pre-dry the coal was effective and reduced the undersize coal moisture content from 5.80% after screening at 5% free moisture content, to 4.35%. This

reduction in moisture by adsorption proved enough to allow stratification to take place and improve screening efficiency. The undersize efficiency increased from 30% to 86% with ceramic pre-drying, with only 30 seconds of contact time prior to screening. This is similar to the 90% achieved when screening with no free moisture present. For screening at 10% free moisture content, the reduction in moisture content was less effective and reduced the average undersize moisture content after screening from 7.06% to 5.83% with 30 seconds contact time prior to screening. It was previously shown by Diedericks *et al.*, (2020:3) that agglomeration takes place at a moisture content above 5%. This was clearly demonstrated by undersize efficiency that increased from 4% to only 70% compared to 90% when screening with no free moisture present. When the contact time was increased from 30 seconds to 120 seconds, the average undersize moisture content reduced to 2.09%. This resulted in an undersize efficiency of 89%, which is similar to screening with no free moisture present.

- The bed depths had negligible effects when dry screening coal with low moisture contents, but the effect increased with increasing moisture content. The increased effect is caused by the free surface moisture causing agglomeration, thus reducing the stratification that takes place. Due to the reduced stratification, the number of presentations of each particle on the screen is greatly reduced with increasing bed depth.

5.2 Recommendation

1. The influence of more specific moisture content intervals on specific particle sizes should be investigated to achieve a better understanding of how moisture influences dry screening of small coal particles.
2. It is important to develop a continuous contact sorption process at pilot plant scale to determine the industrial feasibility thereof. The feasibility study should include the determination of ideal operation – including the feed rates, ceramic-to-coal mass ratio, ceramic size, contact time, and target moisture. The feasibility study should also include a full techno-economic analysis.
3. An effective separation method should be developed to remove ceramic adsorbents from oversize coal particles and the impact of carried-over ceramics on downstream equipment should be studied.
4. The use of airflow to dry coal during screening should be investigated with controlled variables such as humidity and temperature over longer contact times to compare the feasibility of airflow with the feasibility of ceramic adsorbents.

5.3 Contribution

This study contributed by testing the possibility of dry screening small coal particles from Witbank Seam 5 in Mpumalanga, South Africa, and determining the effect of aperture size, moisture, and bed depth on the screening efficiency. The study also contributed by testing the possibility of enhancing dry screening by removing moisture-using airflow from a laboratory instrument airline. Another contribution was to test the possibility of using ceramic adsorbents to pre-dry the coal and, by doing so, enhance the dry screening of small coal particles. The enhancement of dry screening could significantly reduce water consumption and pollution along with reducing the necessity of discarding fine coal to tailings ponds. Hence, the environmental impact of coal processing can be greatly reduced and take the industry one step forward in the drive for cleaner coal.

BIBLIOGRAPHY

- Ackah, L., Akbari, H. & Mohanty, M. 2017. Performance optimization of a new air table and flip-flow screen for fine particle dry separation. *International Journal of Coal Preparation and Utilization*, 40(9), pp.581-603.
- Amaral, R.C.V., Assis, P.S., Braga, E.M.H., Carias, M.D.C., Lemos, L.R., & Silva, G.L.R.D. 2019. Influence of moisture and particle size on coal blend bulk density. *REM-International Engineering Journal*, 72(2), pp.237-242.
- Ameh, E.G., 2019. Geochemistry and multivariate statistical evaluation of major oxides, trace and rare earth elements in coal occurrences and deposits around Kogi east, Northern Anambra Basin, Nigeria. *International Journal of Coal Science & Technology*, 6(2), pp.260-273.
- Barbosa de Lima, A.B., Delgado, J.M.P.Q., Neto, S.F. & Franco, C.M.R., 2016. Intermittent drying: fundamentals, modeling and applications. *Drying and energy technologies*, 63, pp. 19-41.
- Basha, O.M., Morsi, B., & Özer, M. 2017. Coal-agglomeration processes: A review. *International Journal of Coal Preparation and Utilization*, 37(3), pp.131-167.
- Bechtel, A., Christanis, K., Dai, S., DiMichele, W.A., Eble, C.F., Esterle, J.S., Mastalerz, M., O'Keefe, J.M., Raymond, A.L., Valentim, B.V. & Wagner, N.J. 2013. On the fundamental difference between coal rank and coal type. *International Journal of Coal Geology*, 118, pp.58-87
- Campbell, Q.P., Le Roux, M., Peters, E.S., Stiglingh, C. & Van Rensburg, M.J. 2015. Air drying of fine coal in a fluidized bed. *Journal of the Southern African Institute of Mining and Metallurgy*, 115(4), pp.335-338.
- Cardott, B.J. Christanis, K. Crosdale, P. Flores, D. Hamor-Vido, M. Hentschel, A. Kalaitzidis, S. Kus, J. Misz-Kennan, M. Pickel, W. & Rodrigues, S. 2017. Classification of liptinite – ICCP System 1994. *International Journal of Coal Geology*, 169, pp.40-61.
- Cen, K., Chen, D., Jiang, Y., Jiang, X., Liao, H., Ma, Z., Yan, J., Yu, X., & Zhao, H. 2014. The effect of anionic dispersants on the moisture distribution of a coal water slurry. *Fuel processing technology*, 126, pp.122-130.
- Chen, Q. & Wei, L. 2003. Coal dry beneficiation technology in China: The state-of-the-art. *China Particuology*, 1(2), pp.52-56.

Chen, X., Feng, H., Jiang, H., Liu, C., Liu, D., Peng, L., Zhang, L., & Zhao, Y. 2019. A review on the advanced design techniques and methods of vibrating screen for coal preparation. *Powder Technology*, 347, pp.136-147

Dai, S., Eskenazy, G., Finkelman, R.B., French, D., Graham, I.T., Hower, J.C., Ward, C.R., Wei, Q. & Zhao, L. 2020. Organic associations of non-mineral elements in coal: A review. *International Journal of Coal Geology*, 218, pp.103347-103367

Department of Environmental Affairs (South Africa). 2013. *Climate trends and scenarios for South Africa*. https://www.environment.gov.za/sites/default/files/docs/climate_trends_bookV3.pdf. Date of access 29 Oct. 2021

De Korte, G.J. 2015. Processing low-grade coal to produce high-grade products. *Journal of the Southern African Institute of Mining and Metallurgy*, 115(7), pp.569-572.

Diedericks, E.S., Le Roux, M., Campbell, Q.P. & Hughes, N. 2020. Beneficiation of small South African coal using an air dense medium fluidized bed. *International Journal of Coal Preparation and Utilization*, pp.1-14.

Dong, L., Duan, C., Jiang, H., Liu, C., Luo, Z., Wang, Z., Wu, J., Yu, X., Zhang, B., Zhang, C. & Zhao, Y. 2017. Kinematics characteristics of the vibrating screen with rigid-flexible screen rod and the behavior of moist coal particles during the dry deep screening process. *Powder Technology*, 319, pp.92-101.

Duan, C., He, J., He, Y., Luo, Z., Zhao, J. & Zhao, Y. 2015. Separation performance of fine low-rank coal by vibrated gas–solid fluidized bed for dry coal beneficiation. *Particuology*, 23, pp.100-108.

Duan, C., Jiang, H., Pan, M., Qiao, J., Wang, W., Yu, S., Zhao, Y., and Zhuo, Z. 2020 Mechanism of overcoming plugging and optimization of parameters for rigid-flexible coupled elastic screening of moist fine coal. *Powder Technology*, 376, pp.113-125.

Han, Y., Li, X., Tahmasebi, A., Yin, F. & Yu, J. 2013. A review on water in low rank coals: The existence, interaction with coal structure and effects on coal utilization. *Fuel Processing Technology*, 106, pp.9-20.

Hartnady, C.J. 2010. South Africa's diminishing coal reserves. *South African Journal of Science*, 106(9-10), pp.1-5.

He, K., Mi, J., & Zhang, S., 2014. Experimental investigations about the effect of pressure on gas generation from coal. *Organic geochemistry*, 74, pp.116-122.

International Committee for Coal and Organic Petrology (ICCP) 1998. The new vitrinite classification (ICCP System 1994). *Fuel*, 77(5), pp.349-358.

International Committee for Coal and Organic Petrology (ICCP) 2001. The new inertinite classification (ICCP System 1994). *Fuel*, 80(4), pp.459-471.

Karthikeyan, M., Mujumdar, A.S. & Zhonghua, W. 2009. Low-rank coal drying technologies—current status and new developments. *Drying Technology*, 27(3), pp.403-415.

Kaza, M. Raj, M.G. Sah, R. Shanmugam, B.K. & Vardhan, H. 2019a. Evaluation of a new vibrating screen for dry screening fine coal with different moisture contents. *International Journal of Coal Preparation and Utilization*, 1-10.

Kaza, M. Raj, M.G. Sah, R. Shanmugam, B.K. & Vardhan, H. 2019b. Screening performance of coal of different size fractions with variation in design and operational flexibilities of the new screening machine. *Energy Sources, Part A: Recovery, Utilization, and Environmental Effects*, pp.1-9.

Luo, Z., Yang, X. & Zhao, Y. 2017. Dry Cleaning of Fine Coal Based on Gas-Solid Two-Phase Flow: A Review. *Chemical Engineering & Technology*, 40(3), pp.439-449.

Nkolele, A., 2004. Investigations into the reduction of moisture in fine coal by plant tests with surfactants. *Journal of the Southern African Institute of Mining and Metallurgy*, 104(3), pp.171-176.

Peng, Y. Xia, W. and Xie, G. 2015. Recent advances in beneficiation for low rank coals. *Powder Technology*, 277(1):206-221.

Peters, E.S., 2016. Adsorbent assisted drying of fine coal (*Doctoral dissertation, North-West University (South Africa), Potchefstroom Campus*).

South African Weather Service. 2020. *Annual State of the Climate of South Africa*. https://www.weathersa.co.za/Documents/Corporate/Annual%20State%20of%20the%20Climate%202020_19032021121122.pdf. Date of access 29 Oct. 2021.

South African Weather Service. 2021. *Historical Rain*. <https://www.weathersa.co.za/home/historicalrain>. Date of access 29 Oct. 2021.

Van Rensburg, M.J., 2019. A comparison between high airflow drying and adsorption assisted drying for the dewatering of fine coal (*Doctoral dissertation, North-West University (South Africa)*).

ANNEXURES

6.1 Appendix 6.A

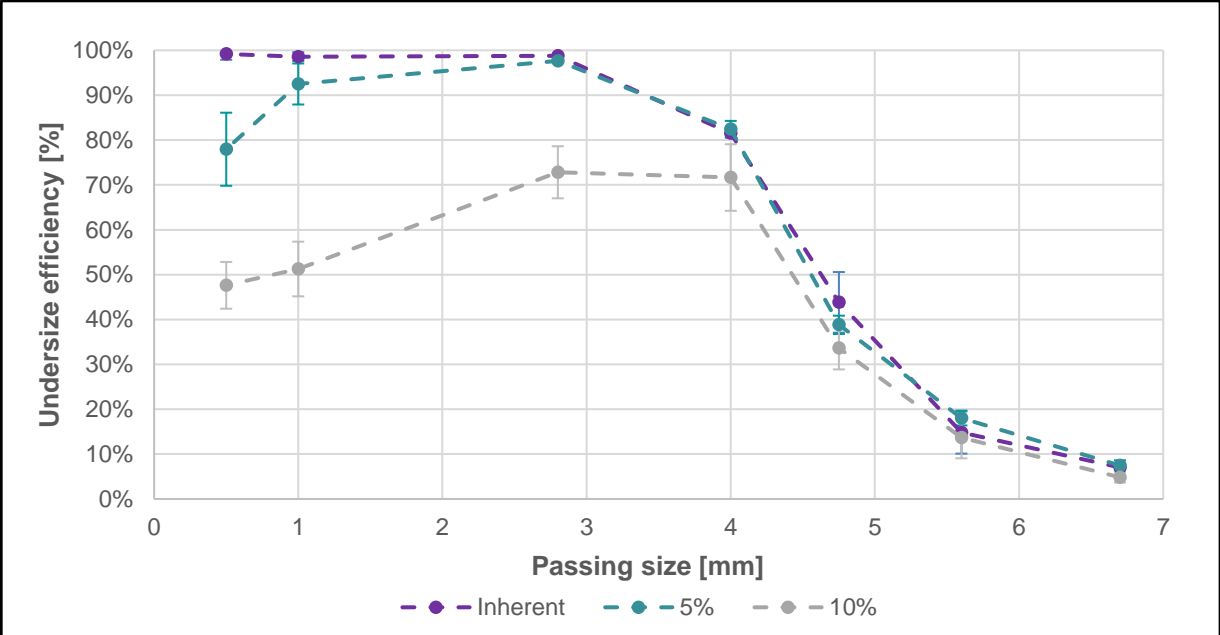


Figure 6.1: Efficiency analysis for each particle size range for basis screening at a low bed depth

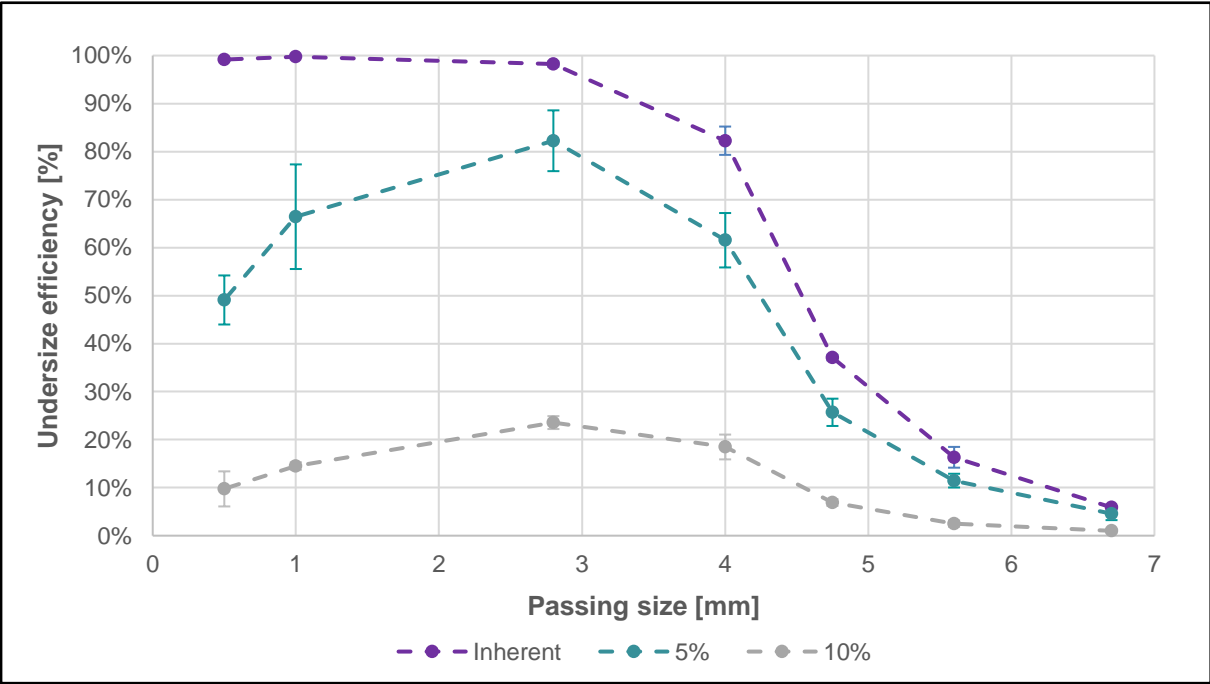


Figure 6.2: Efficiency analysis for each particle size range for basis screening at a high bed depth

6.2 Appendix 6.B

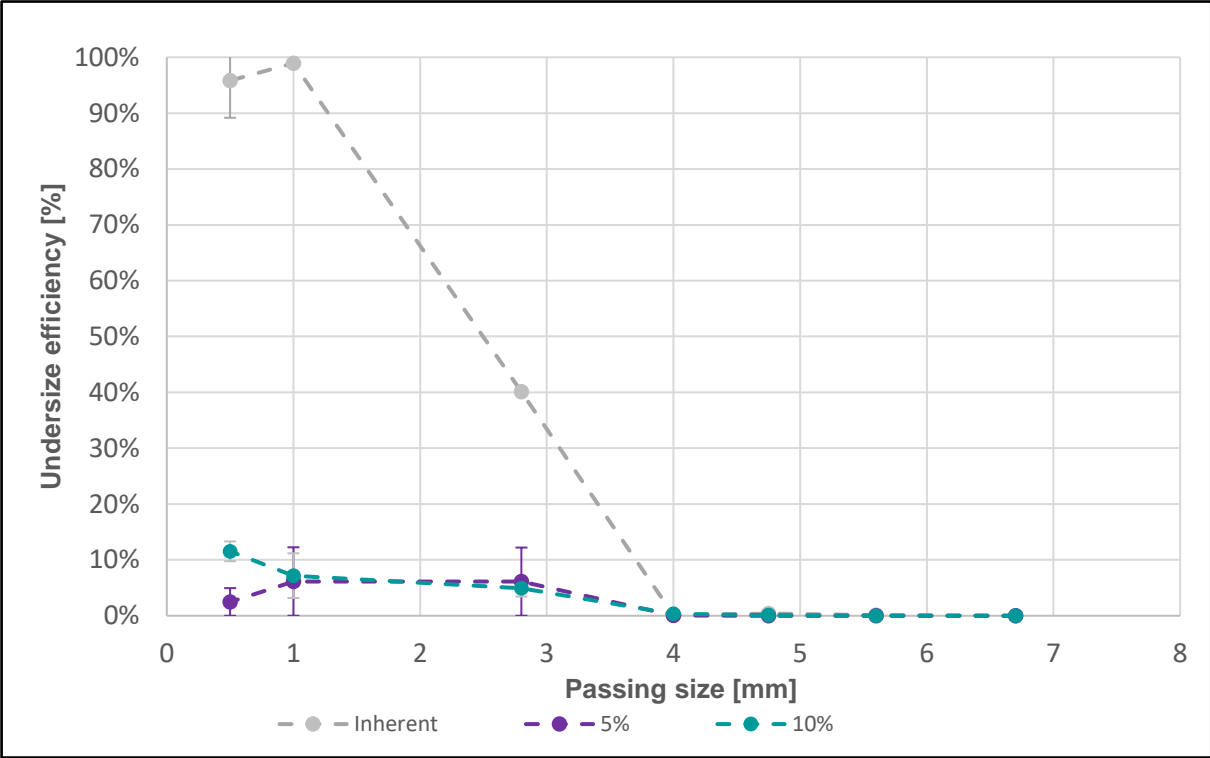


Figure 6.3: Efficiency analysis for each particle size range for basis screening using 2.8 mm aperture size panels at a low bed depth

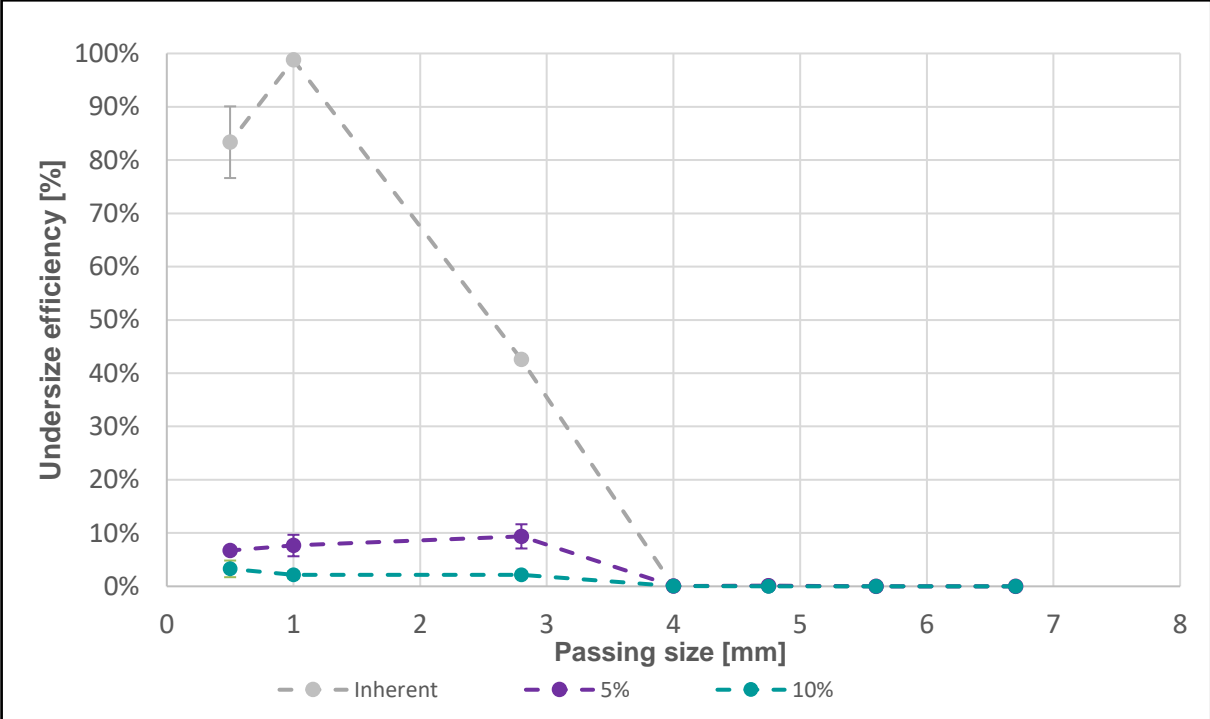


Figure 6.4: Efficiency analysis for each particle size range for basis screening using 2.8 mm aperture size panels at a high bed depth

6.3 Appendix 6.C

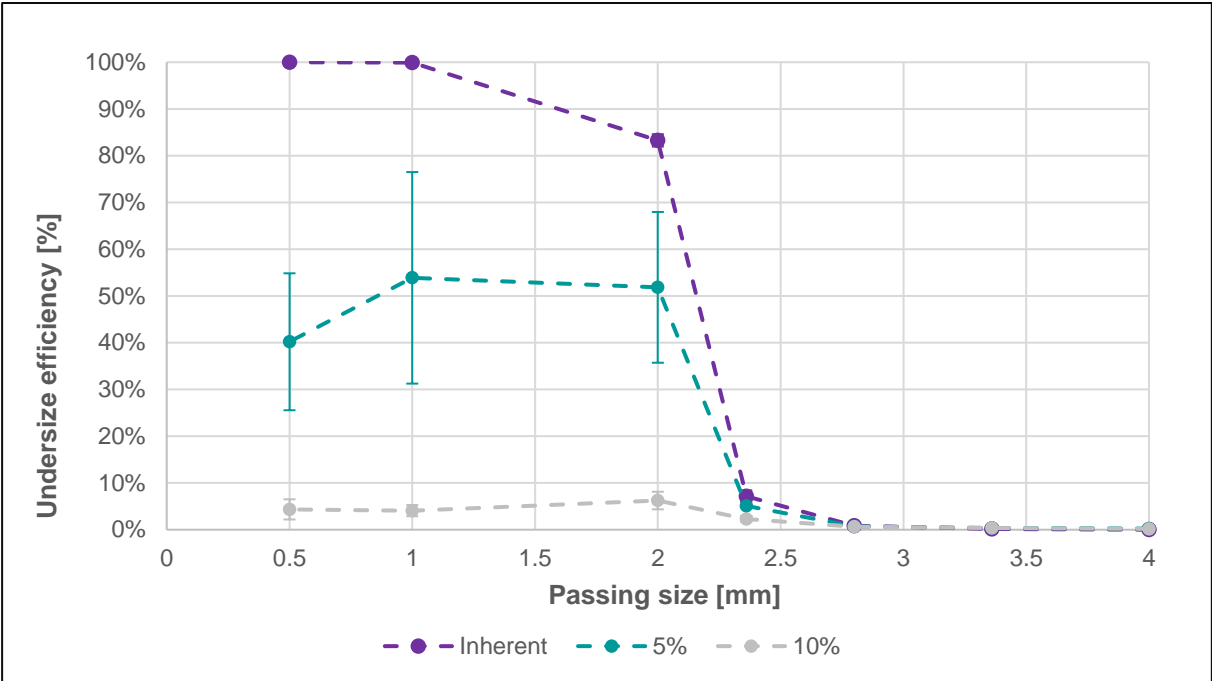


Figure 6.5: Efficiency analysis for each particle size range using the adapted feed at a low bed depth

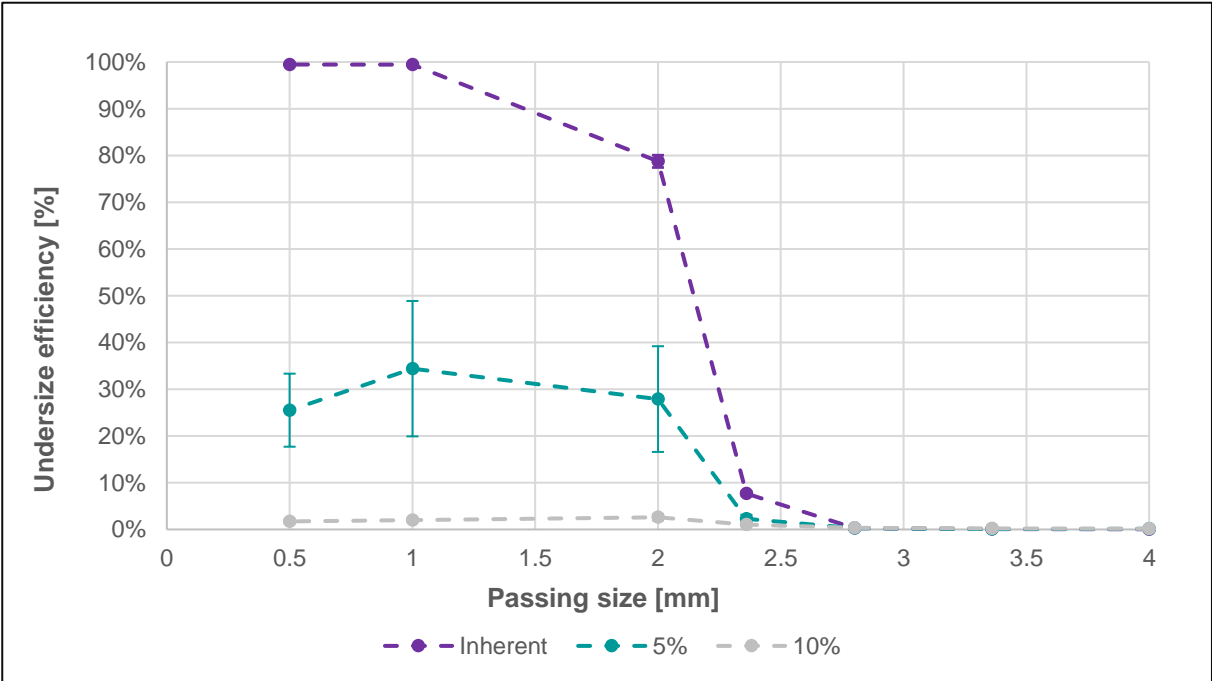


Figure 6.6: Efficiency analysis for each particle size range using the adapted feed at a high bed depth

6.4 Appendix 6.D

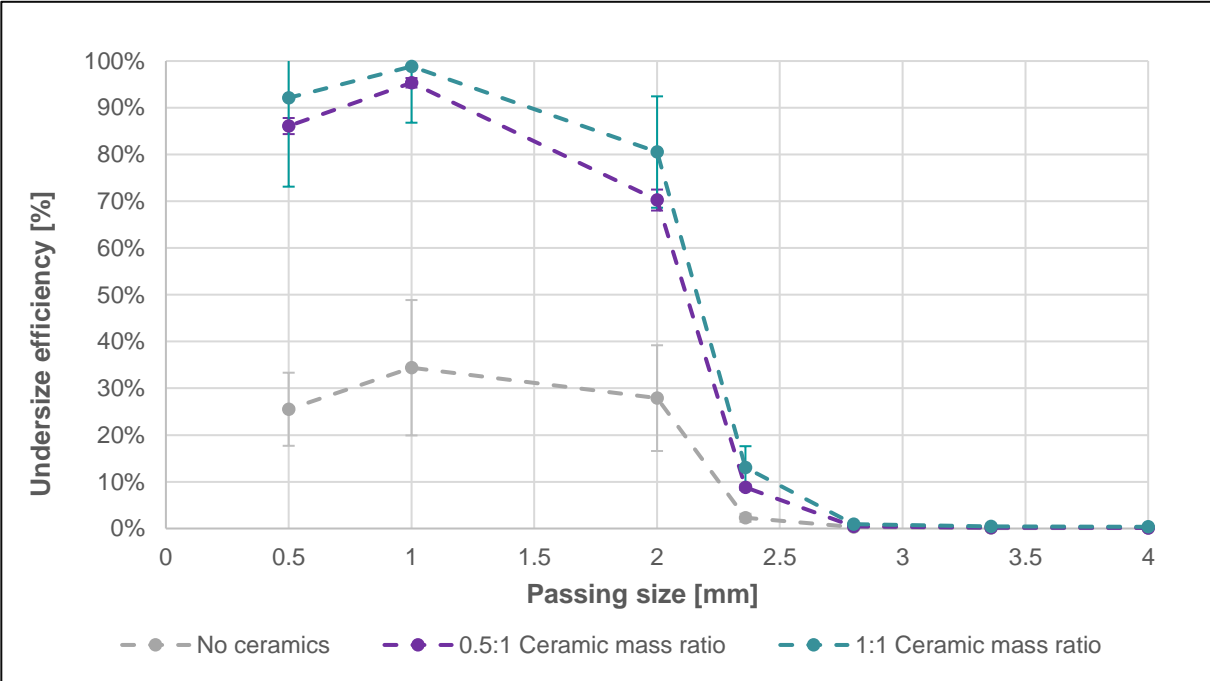


Figure 6.7: Efficiency analysis for each particles size using the adapted feed with the addition of ceramics at 5% moisture content and a low bed depth

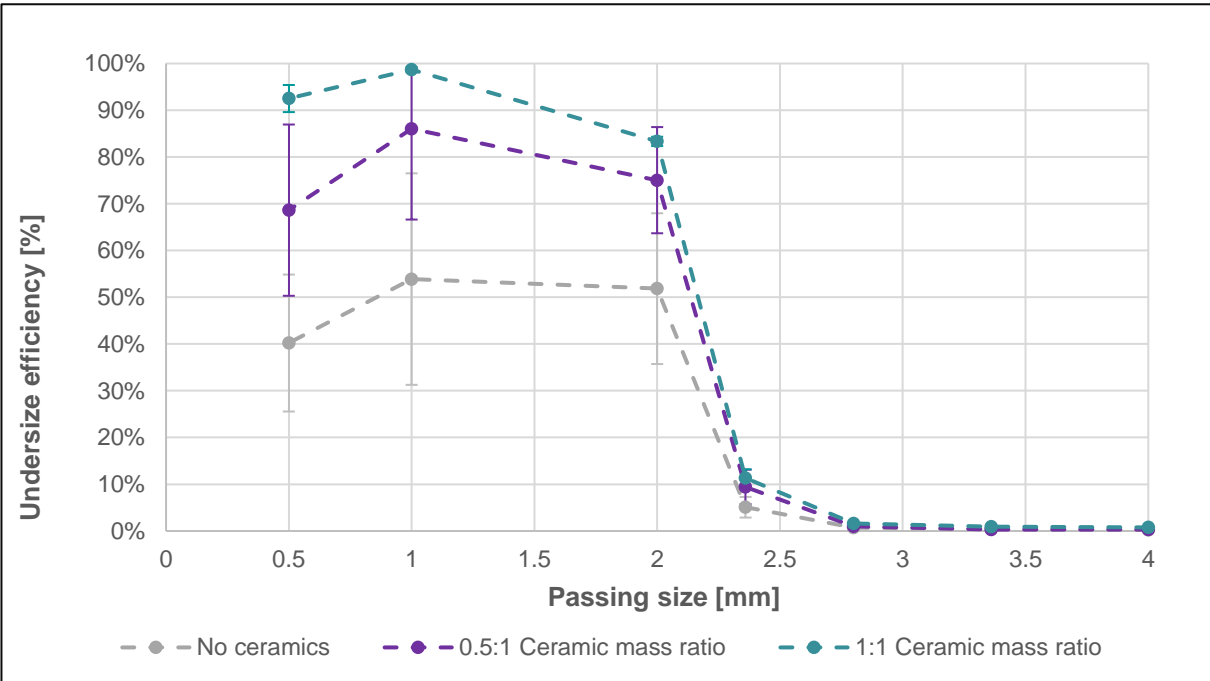


Figure 6.8: Efficiency analysis for each particle size range using the adapted feed with the addition of ceramics at 5% moisture content and a high bed depth

6.5 Appendix 6.E

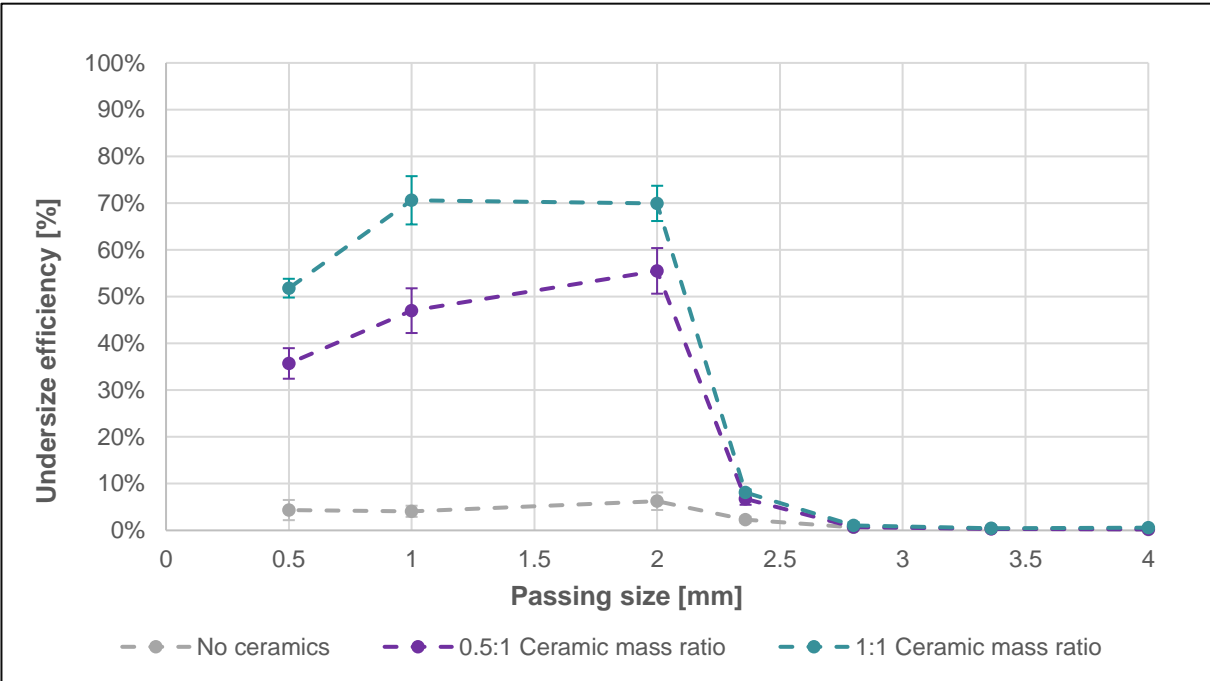


Figure 6.9: Efficiency analysis for each particles size range using the adapted feed at 10% moisture content and a low bed depth

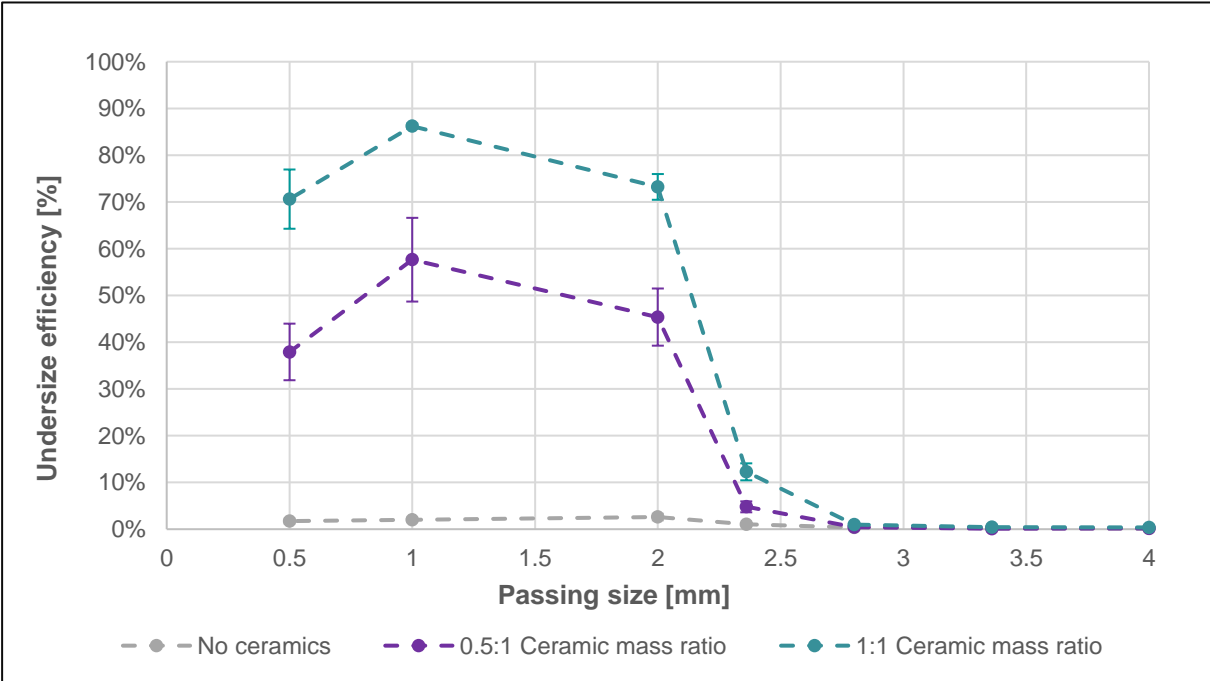


Figure 6.10: Efficiency analysis for each particles size range using the adapted feed at 10% moisture content and a high bed depth